

Summer 2021

Pseudomyxoma Peritonei Derived Cancers: A Novel Study on Growth and Growth Suppression Utilizing Common Colorectal Cancer Agents

Raymond Kenneth Bogdon

Follow this and additional works at: <https://scholarcommons.sc.edu/etd>



Part of the [Biomedical Engineering and Bioengineering Commons](#)

Recommended Citation

Bogdon, R. K.(2021). *Pseudomyxoma Peritonei Derived Cancers: A Novel Study on Growth and Growth Suppression Utilizing Common Colorectal Cancer Agents*. (Master's thesis). Retrieved from <https://scholarcommons.sc.edu/etd/6482>

This Open Access Thesis is brought to you by Scholar Commons. It has been accepted for inclusion in Theses and Dissertations by an authorized administrator of Scholar Commons. For more information, please contact dillarda@mailbox.sc.edu.

Pseudomyxoma Peritonei Derived Cancers: A Novel Study on Growth and Growth
Suppression Utilizing Common Colorectal Cancer Agents

by

Raymond Kenneth Bogdon

Bachelor of Science
Georgia Southern University, 2019

Submitted in Partial Fulfillment of the Requirements

For the Degree of Masters of Science in

Biomedical Sciences

Pathology, Microbiology and Immunology

University of South Carolina

2021

Accepted by:

Traci Testerman, Director of Thesis

Traci Testerman, Reader

Carole Oskeritzian, Reader

Norma Frizzell, Reader

Tracey L Weldon, Interim Vice Provost and Dean of the Graduate School

© Copyright by Raymond Kenneth Bogdon, 2021
All Rights Reserved.

DEDICATION

For my family. Without your continued support none of this would have been possible. For my son, Julian. Although you are too young to understand how important you have been through this process, your happiness and laughter never ceased to raise my spirits. For my wife, Lexie. You have been beside me for every important moment of my life, and words can never express how much you mean to me.

ACKNOWLEDGEMENTS

I would like to thank the University for the incredible opportunity given to me. The faculty of the School of Medicine are world class, both in their experience and willingness to help students. I would specifically like to thank Dr. Traci Testerman, Dr. Carole Oskeritzian, Dr. Edie Goldsmith, Yvonne Hui, and Joann Nagy. Your advice and kindness over the past two years have not gone unnoticed. You have cultivated a culture of family and excellence within the graduate program that elevates students like myself. I am a stronger student and scientist due in no small part to each of you.

ABSTRACT

Pseudomyxoma peritonei is a devastating gastrointestinal disease characterized by the production of mucinous ascites within the peritoneal cavity. Historically, this condition is discovered in the advanced state due to the lack of adequate screening tests and typically presents as an enlarged abdomen and with symptoms of gastrointestinal distress. Treatment for this disease is a combination of cytoreductive surgery and heated intraperitoneal perfusion chemotherapy, but a successful operation does not guarantee full remission of this malignancy. This study focuses on 3 untested variants of PMP cancer, and 2 mucinous colorectal adenocarcinomas that had invaded into the peritoneal cavity. Clinical presentation of the mucinous colorectal adenocarcinomas with peritoneal invasion resembles PMP cancer. Tumor biopsies were obtained through Mercy Medical Center in Baltimore, Maryland. These cancers underwent 2 growth experiments to obtain both the doubling rate and to explore *ex vivo* whether or not each unique proliferative rate impacted chemotherapy agent sensitivities. Four common colorectal cancer chemotherapies were examined and their interactions analyzed alongside 5 cancers. LD50 was calculated for each unique interaction between the chemotherapy agent and the cancers, and this LD50 was compared to clinically relevant plasma concentrations for the agent established through literature searches. The results dictate that Mitomycin C and 5-Fluorouracil were the most effective solitary chemotherapy agents. Oxaliplatin therapy showed some sensitivity, but the required concentration to achieve a 50% reduction in ATP values lay beyond normal plasma concentration parameters. Irinotecan therapy

yielded little sensitivity, showing that Irinotecan was unable to inhibit normal cellular growth even at peak tested concentrations. We decided to modestly explore multi-drug interactions after the disappointing Irinotecan results, combining 5-Fluorouracil and Irinotecan to create a more robust Irinotecan data pool. Results from the combination therapy were more promising, with each cancer showing sensitivity to the treatment. However, calculated LD50 for the Irinotecan concentrations in the multidrug therapy were in excess of clinical accepted plasma concentrations. Multi-drug therapy shows promise in the treatment of these specific cancers, and future experimentation should expand to include other common combination therapies.

TABLE OF CONTENTS

Dedication.....	iii
Acknowledgements	iv
Abstract.....	v
List of Figures.....	viii
Chapter 1: Introduction.....	1
Chapter 2: Materials and Methods	10
Chapter 3: Results	17
Chapter 4: Discussion.....	53
Works Cited	69

LIST OF FIGURES

Figure 3.1 PMP cell line growth experiment. 40,000 cell count	24
Figure 3.2 PMP cell line growth experiment. 10,000 cell count	25
Figure 3.3 ABX 023-1 average ATP values. 10000 cell count growth trial	26
Figure 3.4 PMP 457-2 average ATP values. 10000 cell count growth trial.....	26
Figure 3.5 CO9-1 average ATP values. 10000 cell count growth trial.....	27
Figure 3.6 CO5-1 average ATP values. 10000 cell count growth trial.....	27
Figure 3.7 PMP 501-1 average ATP values. 10000 cell count growth trial.....	28
Figure 3.8 PMP Cell lines treated by MMC therapy at 50,000 cell count	29
Figure 3.9 PMP 457-2 ATP values as treated by MMC 50,000 cell count.....	30
Figure 3.10 PMP 501-1 ATP values as treated by MMC 50,000 cell count.....	30
Figure 3.11 ABX 023-1 ATP values as treated by MMC 50,000 cell count.....	31
Figure 3.12 CO9-1 ATP values as treated by MMC 50,000 cell count	31
Figure 3.13 CO5-1 ATP values as treated by MMC 50,000 cell count	32
Figure 3.14 PMP cell lines treated by MMC therapy. 40,000 cell count trial.....	33
Figure 3.15 ABX 023-1 ATP values as treated by MMC 40,000 cell trial.....	34
Figure 3.16 PMP 501-1 ATP values as treated by MMC 40000 cell trial	34
Figure 3.17 CO5-1 ATP values as treated by MMC 40000 cell trial.....	35
Figure 3.18 PMP Cell lines treated with 5-FU therapy	36
Figure 3.19 CO5-1 ATP values as treated by 5-FU	37
Figure 3.20 PMP 501-1 ATP values as treated by 5-FU	37

Figure 3.21 ABX 023-1 ATP values as treated by 5-FU	38
Figure 3.22 PMP 457-2 ATP values as treated by 5-FU	38
Figure 3.23 CO9-1 ATP values as treated by 5-FU	39
Figure 3.24 PMP cell lines treated by Oxp therapy	40
Figure 3.25 PMP 457-2 ATP values as treated with Oxp	41
Figure 3.26 CO5-1 ATP values as treated with Oxp.....	41
Figure 3.27 CO9-1 ATP values as treated with Oxp.....	42
Figure 3.28 ABX 023-1 ATP values as treated with Oxp.....	42
Figure 3.29 PMP 501-1 ATP values as treated with Oxp	43
Figure 3.30 PMP cell lines treated by Irinotecan therapy	44
Figure 3.31 PMP 501-1 ATP values as treated with Irinotecan.	45
Figure 3.32 ABX 023-1 ATP values as treated with Irinotecan.....	45
Figure 3.33 CO9-1 ATP values as treated with Irinotecan.....	46
Figure 3.34 CO5-1 ATP values as treated with Irinotecan.....	46
Figure 3.35 PMP 457-2 ATP values as treated with Irinotecan	47
Figure 3.36 PMP cell lines treated by 5-FU/Irinotecan combination therapy	48
Figure 3.37 PMP 501-1 ATP values as treated by 5-FU/Irinotecan combination	49
Figure 3.38 CO5-1 ATP values as treated by 5-FU/Irinotecan combination	49
Figure 3.39 CO9-1 ATP values as treated by 5-FU/Irinotecan combination	50
Figure 3.40 PMP 457-2 ATP values as treated by 5-FU/Irinotecan combination	50
Figure 3.41 ABX 023-1 ATP values as treated by 5-FU/Irinotecan combination.....	51

CHAPTER 1

INTRODUCTION

1.1 What is Pseudomyxoma Peritonei

Pseudomyxoma peritonei (PMP) is a rare gastrointestinal disease affecting patients across sexual, geographical, and racial boundaries. Historical data shows that females are more likely to develop PMP than males (60:40), and the development of PMP occurs later in life ⁹. The accepted clinical definition of PMP has evolved since the discovery of the disease over a century ago. The latest data describes PMP as a condition arising from appendiceal neoplasms. There has been evidence of origination from the colon and other regional gastrointestinal organs, but this is a rarity rather than the accepted norm and further classified as invasive colorectal cancer ⁴⁵. The clinical sign of PMP has been the increase in abdominal size in patients, deriving from the endless production of mucin inside the peritoneal cavity. This mucin originates, typically, from an appendicular tumor that has ruptured. Epithelial cells are able to escape from the ruptured neoplasm, and into the peritoneal cavity. Once in the peritoneal cavity these epithelial cells are free to proliferate and produce mucus. It is shown that the cells, suspended in mucus, typically do not bind to surfaces within the cavity due to the lack of adhesion molecules expressed on the cells. This allows the mucus to move seamlessly along the organs as a result of peristalsis and follow gravity's pull to the bottom of the peritoneal cavity ^{44, 55}. Visibly, the patient will present the macro effect of this redistribution with the aforementioned increase in their abdominal area. CT scans are the

most appropriate imaging for the diagnosis of PMP, however the mucinous material itself is difficult to see^{30,3}. Predominantly, early detection of PMP is notoriously difficult due to the lack of dense material inside the peritoneal cavity. Once the disease progresses to a more advanced stage, calcification of material is more readily seen and follows the innate peritoneal fluid motion⁵⁸. However, as the condition advances the specificity of CT is lost and the organs within the cavity are compartmentalized due to the disruptive nature of the growing omental cake⁵⁸. MRI, PET, and PET CT is shown to be less effective as imaging techniques for the detection and progression of PMP. These techniques could be beneficial in the identification of possible metastasis^{3,54}. True confirmation of a PMP diagnosis is performed with laparoscopy and subsequent biopsies^{3,57}.

1.2 Common Mutations Present in PMP

PMP cancers are known to have numerous mutations which pathologically can determine the degree of aggression of the disease. PMP is divided into two types: disseminated peritoneal adenomucinosis (DPAM) or peritoneal mucinous adenocarcinomas (PMCA). DPAM is considered the less aggressive type of PMP. PMCA, however, is shown to invade organ tissue causing significant damage and have high levels of epithelial proliferation. KRAS gene mutations are common, while GNAS gene mutations are rarer^{47,43}. Often, a combination of KRAS and GNAS mutations are found within PMP cancers. Noguchi found evidence of TP53 mutations within PMCA patient samples, but none within DPAM samples. It was theorized that the TP53 mutation promotes the aggressive malignant nature of PMCA⁴⁷. TP53 is a common mutation in cancer and is responsible for Li-Fraumeni syndrome. P53 activates the expression of p21 after recognition of nuclear damage^{14,35}. It was also shown in a study performed by

Guidos et al that p53 - scid deficient mice are unable to stop cell cycle progression with double strand breaks in DNA. With the checkpoint rendered ineffective, the mice developed disseminated pro-b or immature T cell lymphoma ²¹.

KRAS is an oncogene, and studies have shown that KRAS mutations are apparent in up to 45% of colorectal cancers. KRAS is responsible for the p21 protein, a GTPase responsible for EGFR-signaling intracellularly ^{61,32}. When mutated, KRAS GTPase activity is inhibited and p21 is locked in the GTP bound form. When locked into this active form, cell growth is accelerated by activated proliferative pathways ^{61,4,50}.

It is common to detect mutations in the GNAS gene with mucinous neoplasms of the appendix, colon, and pancreas ¹⁷. It is then not surprising that PMP, which is known to typically originate from mucinous neoplasms of the appendix, would in turn also have a propensity for GNAS gene mutations. The GNAS gene encodes for a guanine nucleotide-binding protein α ($G\alpha$) subunit. This protein receives signals from G-protein coupled receptors and passes this signal to adenylyl cyclase which in turn influences the expression of cyclic adenosine monophosphate ³⁶. There are two significant mutation variants seen in PMP patients both located on chromosome 20. A single nucleotide mutation of thymine to adenine causes a shift from the wild type arginine amino acid to cysteine and histidine. This leads to a decrease in GTPase activity due to the mutated structure. The mutated protein is unable to effectively hydrolyze GTP, thereby staying within the active status and stimulating subsequent pathways ³⁶. The Nishikawa study validated the relationship between GNAS mutations and mucin production experimentally in CRC by measuring elevated levels of cAMP, MUC2, and MUC5AC ⁴⁶. ³⁶. Elevated cAMP levels are theorized to stimulate both the cAMP response element

bind protein and activating transcription factor, which binds to mucin genes to increase mucin expression ^{62, 36}.

1.3 Cancer Growth

Cellular growth is ubiquitous nearly everywhere within the human body. Proliferation of cells ensure a timely and productive turnover of older cells to that of newer and healthier cells. However, cellular growth is checked by two synergistic features of multicellular organisms, contact inhibition of proliferation and contact inhibition of motility. Typical human cells do not proliferate endlessly after reaching an appropriate cellular density, with some exceptions of certain normal physiological variables ^{48,41}. Cell to cell contact activates numerous signaling pathways including E-cadherin proteins ⁴². Studies have shown that cancerous cell lines fail to express E-cadherin at detectable levels, where as normal healthy cells have abundant E-cadherin proteins at lesser cellular densities ⁵³. Cancer metastasis hinges upon E-cadherin absence in cells. The lack of this critical membrane protein allows for cells to invade surrounding tissue, thereby bypassing contact inhibition of locomotion ⁴². Due to the extreme proliferation rate of cancerous tumors, chemotherapeutic agents have been devised to capitalize and preferentially attack cells that divide at a higher rate than surrounding tissue. The high division rate, and the hypoxic conditions of solid-state tumors, leaves them open to therapeutic intervention.

1.4 Treatment of PMP Cancer Historically

Despite the heroic efforts of countless surgeons and physicians a diagnosis of PMP does not always have positive outcomes. While PMP shares many similarities with other malignant cancers, it has been shown historically that PMP requires a multi-

targeted approach. The treatment draws inspiration from numerous sources, and can be best described as a combination of aggressive cytoreductive surgery (CRS) and Heated intraperitoneal perfusion chemotherapy (HIPEC). Studies have shown that in patients suffering with PMP, CRS without HIPEC is far less effective than the combination. CRS will reduce all visible signs of malignancy; however, the procedure could also allow some malignant cells to burrow deeper within the patient's abdomen or pelvis if not all cancer cells are removed. In addition, malignant cells that have already invaded into the tissue would not be removed by CRS alone⁵⁶. This in turn could lead to additional negative physiological effects for the patient's gastrointestinal or renal system as a result of the spreading cancer. Administration of HIPEC after CRS has been shown to reduce this possibility⁵⁶. CRS is utilized in the treatment plans for both benign and malignant non-PMP tumors. The intention is to remove all visual evidence of the PMP derived mucin and epithelial cells within the patient's abdominal cavity. After successful CRS, the patient is administered HIPEC while in the surgical theatre. Chemotherapeutic drugs are heated to 41°C and are introduced into the patient's peritoneal cavity. It is shown that hyperthermic temperatures increase the efficacy of therapeutical agents, and in cases of more traditional CRC reduce the rate of tumor reoccurrence^{56,25}. Similar studies have shown that hyperthermic conditions alone will negatively impact the proliferation of CRC cells²⁵. The heated drug bathes the internal cavity of the patient, and is subsequently removed by suction. This therapy is more effective than traditional systemic chemotherapy due to the lack of vascularization within the cavity itself⁴⁴. HIPEC without CRS is shown to be less effective than the combination of both procedures. Chemotherapeutics, when given in this manner, rely on passive diffusion to reach

malignant cells and studies have shown that this penetration ranges from the surface cells to possibly 3mm³⁸. Administration of chemotherapy drugs in this manner allows for maximum coverage of the affected areas within the peritoneal cavity. The concentration of drugs used in HIPEC are typically higher than that of traditional systemic chemotherapy with the same drugs. Due to the lack of vascularization within the peritoneal cavity, there is low risk of the full therapeutic dose invading systemic circulation⁶⁴. This anatomical feature provides a distinct advantage to HIPEC, but also restricts the effectiveness of traditional systemic chemotherapy. Without a direct flow of arterial blood, it would be otherwise impossible for systemic chemotherapy to provide a meaningful effect for PMP. CRS and perioperative HIPEC do not guarantee a successful remission of this cancer, and, in reality, relapse is common for these patients.

1.5 Chemotherapeutics Used in PMP

Chemotherapeutic drugs are varied and vast in numbers. However, to date there has not been an exhaustive study on the effects of common chemotherapy drugs on PMP derived cancers. That was the focus of this study. Four drugs were chosen due to their prevalence of use for gastrointestinal or colorectal cancers (CRC).

Mitomycin C (MMC) is a commonly used therapeutic in HIPEC chemotherapy procedures. MMC causes a lethal crosslinking of complementary DNA strands, and is an effective non-growth specific antibiotic agent⁶³. However, it is the compound's relative sensitivity to carbon monoxide or oxidative stress that allows for a more selective focus in the treatment of cancer. Due to the lack of both carbon monoxide and oxygen, solid tumors are a prime location for the generation and maintenance of reactive drug metabolites from MMC³⁰. At a high concentration MMC is able to kill cells in normoxic

conditions, and this is of critical importance when determining an appropriate therapeutic dose ³³.

The mechanism of 5-Fluorouracil (5-FU) is not completely understood; however, it is assumed that the introduction of therapeutically active metabolites interferes with the synthesis of DNA during the S phase. 5-FU is an antimetabolite, and, along with the folate cofactor, binds to thymidylate synthase. This in turn inhibits the formation of thymidylate, and inhibits the synthesis of both DNA and RNA ⁶³. 5-FU has a long history of use in various types of cancers: bladder, CRC, and skin cancers amongst others. 5-FU is used in specialized manners like HIPEC as part of multi drug treatment plans yielding promising results for patient 5 to 10-year survival ratings. With respect to advanced CRC, 5-FU as the primary drug is shown to have a 10-15% survival rate, yet when combined with Oxaliplatin boosts survival rates up to 40% ¹⁸.

Oxaliplatin (Oxp) is a widely used chemotherapy agent used for CRC, advanced CRC, gastric, and bladder cancers ^{63, 12, 22}. In vivo, Oxp is metabolized into active metabolites which bind to both guanine and cytosine nucleotides in DNA. This binding leads to crosslinking within the DNA, and inhibits nuclear functionality within the cell ⁶³. Oxp is a platinum-based compound and, while its therapeutic effects cannot be argued, it is plagued with hypersensitivity reactions. These reactions can vary from mild, such as chills or fever, to more severe like thrombocytopenia ^{2, 15}. Numerous studies show effective means to mitigate Oxp induced toxicities. Oxp, while effective as a solitary drug, is often used as part of a multi-drug treatment for CRC known as FOLFOX. FOLFOX is a combination therapy consisting of 5-Fluorouracil, leucovorin, and

Oxaliplatin. FOLFOX is shown to be more effective than Oxaliplatin monotherapy, and with less toxicity ²².

Irinotecan is a chemotherapy agent commonly prescribed for CRC, pancreatic and lung cancer ¹⁰. Irinotecan is a pro-drug transformed, in vivo, to SN-38 which is the active cytotoxic agent. SN-38 is 100-1000 times more potent than the un-modified Irinotecan, and is the mitigating factor responsible for dose limiting toxicities ^{63, 10, 22, 28}. Irinotecan and SN-38 impact the cell's ability to replicate DNA by binding to the topoisomerase I DNA complex. Topoisomerase I mitigates supercoiling of DNA post replication fork by cleaving a single strand. This chemotherapy agent, topoisomerase I, and DNA super complex cause lethal double strand breaks within the cell DNA. These double strand breaks lead to cellular apoptosis ²⁸. Irinotecan is a part of FOLFOXIRI, a derivative of FOLFOX which contains 5-FU, leucovorin, oxaliplatin, and Irinotecan. This treatment is extremely effective although inducing neutropenia and peripheral neurotoxicity ^{52, 22}.

1.6 Mucinous Colorectal Cancer

In addition to true PMP cancers, this study also includes 2 mucinous colorectal cancers that had invaded the peritoneal cavity of patients: CO5-1 and CO9-1. Visually, both the PMP cancer and mucinous adenocarcinoma appear similar. Mucinous colorectal adenocarcinomas typically produce large quantities of MUC2 and MUC5AC mucins ^{59, 39, 23}. Mucinous colorectal adenocarcinomas was found to be present in 38.5% of CRC patients in the Leopoldo study, but statistics vary through literature³⁴. The location of the mucinous CRC tumor is predicative of severity of outcomes, with more distal colon locations yielding a far bleaker prognosis. There is differential gene expression between the proximal and distal colon MUC, and this leads to distinct histological features³⁴. The

CO9-1 biopsy was removed from the cecum, while the CO5-1 original biopsy was removed from the sigmoid colon of PMP patients.

1.7 Experimental Intent

These experiments were designed from the historical precedence of chemotherapeutics used as treatment for GI or CRC localized cancers. The intention of this study is to provide dose response curves to PMP cell line cancer, and determine the LD50 of their interactions. A multi-drug therapy was devised to test the synergy between 5-FU and Irinotecan and to provide insight for future experimentation with other multi-drug therapies. These cancers were acquired from patients who suffer from unique instances of PMP through Mercy Medical Center in Baltimore, Maryland.

CHAPTER 2

MATERIALS AND METHODS

2.1 Cell Culture

In this study 5 cancers were managed and tested: CO5-1, CO9-1, PMP 501-1, PMP 457-2, and ABX 023-1. The patients, prior to biopsy removal, had no history of either radiation therapy or HIPEC. Within this study the prefix ABX designates that the PMP cell line was obtained from a patient who underwent antibiotic therapy with lansoprazole, amoxicillin, and clarithromycin. MS CO5-1 F3 (CO5-1) was a human mucinous adenocarcinoma cell line xenografted into an immune deficient mouse model and subsequently cultured *in vitro*. CO5-1 was removed from the mucin within the peritoneal cavity, but originated from the sigmoid colon of a 61-year-old female patient. The patient had undergone 2 separate cycles of FOLFOX/Avastin chemotherapy prior to biopsy removal. CO9-1 was a moderately differentiated mucinous adenocarcinoma from a 48-year-old male patient, originating from the cecum but removed from the omental fat. The patient received three chemotherapy cycles: FOLFOX, Xeloda/Oxaliplatin, and FOLFOX/Avastin prior to biopsy. PMP 501-1 was removed from the peritoneal cavity of a 70-year-old female patient. Prior to biopsy, this patient also had no history of chemotherapy. PMP 501-1 was a DPAM type PMP cancer that was well differentiated. This cancer had evidence of extracellular mucin organization. PMP 457-2 was a DPAM type PMP cancer removed from the peritoneal cavity of a 53-year-old male patient with no history of chemotherapy. In addition to extracellular mucin organization, there was

evidence of strips of mucinous epithelium within the sample. ABX 023-1 was a PMCA-S type PMP cancer which was moderate to poorly differentiated. The biopsy was removed from the pelvic peritoneum of a 40-year-old male patient, with evidence of fibrous tissue in organizing extracellular mucin. Prior to biopsy this patient had undergone a cycle of FOLFOX/Avastin.

Each PMP cancer cell line was cultured in T25 flasks and passaged every 3 days. The flasks that had reached 90% confluency, after a visual inspection utilizing light microscopy, were subcultured into new T25 flasks. The T25 flasks were stored in an environmentally controlled incubator which maintains total atmospheric CO₂ at 5% and 37°C. The used media was aspirated and adherent cells rinsed with 3ml of 1x Phosphate Buffered Saline (PBS) solution. The 1x PBS was then aspirated, and 0.6mL of trypsin (0.05% trypsin/EDTA from Thermo Fisher) was added to the T25 flask. Each flask was then returned to the incubator. After 4 minutes, the flasks were removed from the incubator and checked for adequate detachment. After confirming detachment of the monolayer, 2.7mL of PMP medium are added to each T25 flask. The PMP medium was a solution of: Corning Ham's F12 Nutrient Mixture (Ref 10-020-CV), 10% heat-inactivated fetal bovine serum, 10µg/ml recombinant human insulin, and 1x ampicillin/streptomycin. A mechanical pipette was used to de-clump the cells and resuspend the cells and 1mL of this solution was added to the new T25 flasks containing 5 mL growth medium.

The cancer lines that had not achieved confluency were fed with 6 mL of new PMP. These cell lines are visually inspected each week to determine the degree of

confluency, and once confluent the cancer cells are transferred into new T25 flasks utilizing an identical protocol as above.

2.2 Cell Counting

The cancer cell lines were counted prior to any experimentation. 30uL of trypan blue was added to a sterile microcentrifuge tubes containing detached tumor cells. The microcentrifuge tube is mixed by tapping, and 10uL of the mixed solution is pipetted onto a hemocytometer. The total number of cells counted within the hemocytometer were multiplied by 2, divided by four, and then multiplied by 10000. The desired cell count in the experiment was then divided by this calculated number.

2.3 Plating PMP Cancer Cell Lines

Each well of the 96 well plate was calculated to a combined total volume of 100uL. This is a combination of both the PMP cell line and PMP Media. To initially plate each 96 well plate, the cancer cell lines were calculated, as previously stated, to determine the appropriate volume for each well. This volume was then subtracted from the total volume of 100uL to determine the volume of PMP media. Using a multichannel pipette, the appropriate volume PMP media was added to each well. Subsequently, the appropriate volume of cancer cell solution is added to each well. Once plated, the time was recorded and the plate incubated in an atmosphere of 5% CO₂ at 37°C for 24 hours. This time table was designed to allow the cancer cells to attach to growth plate on the bottom of the well and proliferate to the desired cell count.

2.4 Dosage and Treatment

At the end of 24 hours, the 96 well plate was removed from the incubator and visually inspected under a light microscope to verify cell attachment at the bottom of the

well. The media within each well was aspirated with the vacuum set up, with careful attention to not disrupt the cell attachment at the bottom of each well. Four chemotherapeutic drugs were tested across a range of dosages: Mitomycin C (MMC), 5-Fluorouracil (5-FU), Oxaliplatin (Oxp), Irinotecan, and 5-FU/Irinotecan combination. DMSO was the vehicle used to dissolve MMC, 5-FU, and Irinotecan. A vehicle control was created in these specific cell lines to monitor DMSO toxicity to the cancer cells. Sybr green was also added to each dose to measure cell proliferation. Sybr green was prepared in a 10% concentration solution for these experiments with PMP media + antibiotics. Each well received 50ul of the appropriate cancer therapeutic solution including all control wells. Each PMP cell line were subjected to 48 hour treatments with each tested chemotherapy, and then subsequently scanned for dsDNA and ATP values using the Biotek Synergy 2 microplate reader. The chemotherapy agents were obtained through Caymen Chemical Ann Arbor, Michigan.

Initial experiments used Mitomycin C (MMC) concentrations ranging from 1µg/ml-100µg/ml. Based on these results, concentrations between 1 µg/ml and 5 µg/ml were used for subsequent experiments. MMC was prepared in both a 1mg/ml and 10mg/ml stock solution for these experiments using 100% DMSO as a solvent. The low dose experimentation was performed under both 50000 and 40000 cell counts.

The initial 5-Fluorouracil (5-FU) experiment dose concentrations ranged from 500nM to 500µM. Based on these results, the final dose concentrations were 35µM to 500µM. DMSO was prepared in a 1.3% concentration solution from 100% DMSO using PMP media + antibiotics. 5-FU was prepared in a 1mM concentration using a 10mg/ml 5-

FU stock solution (76.9mM) and PMP media. The 5-FU stock solution was prepared using 100% DMSO as a solvent.

Oxaliplatin (Oxp) dose concentrations ranged from 40 μ M to 120 μ M. The Oxaliplatin stock solution was prepared using deionized water creating a 5mg/ml solution (12.5849mM).

Irinotecan dose concentrations ranged from 20 μ M to 100 μ M. The Irinotecan stock solution was prepared using 100% DMSO as the solvent. Ultimately, the Irinotecan stock solution was 20mg/ml (34.089mM).

The 5-FU/Irinotecan combination trial had one range of drug concentrations. PMP cell lines were initially treated for 6 hours with 100 μ M 5-FU. A 5-FU DMSO vehicle control was created in accordance with the 5-FU protocol. After 6 hours, the 5-FU treatment was aspirated from the 96 well plate with a vacuum set up with the exception of the 5-FU DMSO vehicle control. The 5-FU DMSO vehicle control was allowed to remain through the entire 48 hours. Irinotecan was then added to the 96 well plate in accordance with the Irinotecan protocol with the exception of the 20 μ M concentration. Background control wells were created with both vehicle controls. The Irinotecan treatment continued for 42 hours in order to mirror the 48-hour treatment performed with previous dose response curves.

2.5 dsDNA Assay

. At the end of the experiment, the 96 well plate was removed from the incubator and wrapped in aluminum foil for transport to the microplate reader. The 96 well plate was inserted into a Biotek Synergy 2 microplate reader. The program read fluorescence within the 520nm wavelength of light and calculated a total fluorescent value per well.

The plate was then wrapped in aluminum foil for transport back to the laboratory for additional testing. The background control well numbers were averaged, and then subtracted from each raw number to provide the data for analysis. The numbers were normalized to the vehicle control well to calculate dsDNA increase/decrease on Microsoft Excel. The data was then entered into Graph Pad Prism, for statistical analysis and graphing.

2.6 ATP Assay

50µl of Promega BacTiter-Glo (BTG) was added to each well of the 96 well plate in a 1:1 volumetric ratio. After the addition of BTG the plate was once again covered in aluminum foil. The covered plate was then mixed for 5 minutes at a moderate pace with an orbital shaker. The plate was then read by the Biotek Synergy 2 microplate reader which measured the luminescence within each well to assign values to the ATP content. The background control well numbers were averaged, and then subtracted from each raw number to provide the data for analysis. The numbers were equalized to the vehicle control well to show proportionality of ATP values on Microsoft Excel. The data was then entered into Graph Pad Prism, where all statistical analysis and graphing took place.

2.7 Proliferation Trials

The proliferation experiment evolved through two unique cell counts utilizing an identical procedure: 40,000 and 10,000 cell counts. Each of the PMP cell lines were plated with the appropriate initial cell count using the same methods as outlined earlier. A 96 well plate was prepared with 5 distinct cancer cell lines: PMP 501-1, PMP 457-2, CO9-1, CO5-1, and ABX 023-1. Each cell line was analyzed in triplicate. The plate was labeled with the time of plating, and a background control well was created using only

PMP media + antibiotics. Each day had a unique control well to verify the sterility of the PMP medium. The 96 well plate was then stored for 24 hours in an environmentally controlled incubator at the same parameters as previously mentioned. Every 24 hours for 5 (40,000 cell experiment) or 6 (10,000 cell experiment) the 96 well plate was removed from the incubator and 100 μ l BTG was added in a 1:1 ratio with the initial well volume. The 96 well plate was then wrapped in aluminum foil, and placed on an orbital shaker at a moderate speed for 5 minutes. The plate was then read by the Biotek Synergy 2 microplate reader utilizing the same ATP program as utilized in the ATP assay. Each set of triplicates indicated 24 hours of cell proliferation, and for each day this protocol was repeated. At the end of the 6-day experiment, the numbers were normalized to the 24 hour time point of ATP values with the average background value subtracted from the raw data values on Microsoft Excel. The normalized numbers were then entered into Graph Pad Prism where all subsequent statistical analysis and graphing took place.

2.8 Statistical Analysis

For each chemotherapy experiment *t*-Tests were performed between the control and subsequent concentration points. For the 10,000 cell growth experiment *t*-Tests were performed between the 24 hour baseline and each subsequent 24 hour point. P values were calculated and displayed on each graph where appropriate, using $p < 0.05$ as the cut off for significance. SEM was calculated to provide error at both the control and for each concentration point for the chemotherapy experiments.

CHAPTER 3

RESULTS

3.1 40,000 and 10,000 Cell Count Growth Experiment

The first growth experiment was initially seeded in each well with 40,000 cells (Fig 3.1). Over 72 hours ATP values were unremarkable with the exception of PMP 457-2 which had a recorded 26.2% ($\pm 18.4\%$) increase from control. ABX 023-1 had the largest growth in this experiment by 96 hours with a 38.7% ($\pm 10.7\%$) increase in ATP values. From 96 to 120 hours each of the cancers had a reduction in ATP values. The most extreme reduction occurred with PMP 457-2, which fell 52.1% between 96 and 120 hours. CO9-1 ATP values at 120 hours were the smallest in the experiment, a 43.8% ($\pm 3.87\%$) reduction from control. A second growth experiment was devised with an initial density of 10,000 cells per well. Over 72 hours ATP values consistently increased for all cancers (Fig 3.2). ABX 023-1 ATP values increased more than 2-fold increase by 72 hours and reached peak growth by 96 hours, with a 147.8% ($\pm 28.7\%$) increase from baseline values (Fig 3.3). At 120 hours, however, ABX 023-1 suffered a large drop in ATP values falling 72.9% (± 16.7) below the baseline 24 hour mark. At the 144 hour mark ATP values continued to decrease, a 82% ($\pm 12.4\%$) reduction from control. Significance was present at each time point in the experiment. PMP 457-2 consistently measured increasing ATP values until the 72 hour mark, measuring peak growth as a 89.6% (± 4.37) increase from baseline (Fig 3.3). From 96 hours ATP values fell but maintained baseline levels, and by 144 hours these values fell 6.63% ($\pm 8.1\%$) below

control. Significance was observed from 48 to 96 hours. CO9-1 ATP values increased until reaching peak growth at 72 hours, a 96.7% ($\pm 12.9\%$) increase from control (Fig 3.5). ATP values were maintained through 96 hours, before falling from control in excess of 90% at 120 hours, 92.7% ($\pm 3.47\%$), and 144 hours 95.5% ($\pm 4.51\%$). In addition, significance was present at each time point. CO5-1 ATP values had reached peak numbers by 72 hours, a 163.6% ($\pm 19.6\%$) increase from control (Fig 3.6). Through 96 hours ATP values remained as a two-fold increase from the baseline, but these values began to fall by 120 hours with a 45.2% ($\pm 5.18\%$) increase from control. At 144 hours ATP values fell below that of control, an 8.69% ($\pm 3.63\%$) reduction. Significant differences were present in this experiment through 120 hours. PMP 501-1 ATP values rose until 72 hours where it eclipsed a two-fold increase, 105.8% ($\pm 2.25\%$) from control (Fig 3.7). Beginning at 96 hours and lasting through 120 hours, ATP values gradually fell to a 37.9% ($\pm 28.1\%$) increase compared to baseline. At 144 hours, however, these values precipitously fell 60.9% ($\pm 23.0\%$) from control values. Significant difference was present through 96 hours in this experiment.

3.2 Mitomycin C 50,000 Cell Count Experiment

Of the five cancers, only ABX 023-1 and PMP 501-1 showed an average ATP increase from control at 1 μ g/ml MMC: 44% ($\pm 38.1\%$) and 10.3% ($\pm 24.8\%$) respectively (Fig 3.8). PMP 457-2 ATP values declined significantly at 2 μ g/ml and higher concentrations of MMC (Fig 3.9). At the highest concentration PMP 457-2 had a 77% ($\pm 10\%$) reduction from control. PMP 501-1 ATP values consistently declined over the dose curve, reaching a 63.6% ($\pm 18.8\%$) reduction from control at 5 μ g/ml ($P < 0.05$ vs control) (Fig 3.10). ABX 023-1 ATP values dipped below that of control at

concentrations of MMC greater than 4µg/ml (Fig 3.11). Significant difference was only observed at 5µg/ml, with a 52.5% ($\pm 16.8\%$) reduction from control. At concentrations greater than 1µg/ml MMC, CO9-1 ATP values are below that of control (Fig 3.12). Significant difference is only present at 3µg/ml and greater concentrations, and ATP values fell below 50% of control by 4µg/ml. CO5-1 had consistently declining ATP values as the concentration of MMC increased, with significant difference present at 3µg/ml and greater concentrations (Fig 3.13). ATP values were below 50% of control by 4µg/ml, and at maximum concentration CO5-1 had a recorded 60.6% ($\pm 13.3\%$) reduction from control.

3.3 Mitomycin C 40,000 Cell Count Experiment

ATP values for each of the 3 tested cancer cell lines consistently fell as the concentration of MMC increased (Fig 3.14). Additionally, by 3µg/ml MMC, each of the cancer ATP values was below 50% of its control value. A significant difference was observed at each drug concentration for ABX 023-1, and at maximum concentration there was a 66.5% ($\pm 10.2\%$) reduction from control (Fig 3.15). PMP 501-1 ATP values were the lowest at 4µg/ml, a 74.1% ($\pm 7.02\%$) reduction from control, but slightly increased by 4% at maximum concentration (Fig 3.16). Significance was present at concentrations of 2µg/ml and greater. (Fig 3.17). The ATP values for CO5-1 remained consistent from 3-4µg/ml, but had the largest total reduction at maximum concentration 80.6% ($\pm 7.68\%$) from control (Fig 3.17). Significance was present at each drug concentration.

3.4 5-Fluorouracil Experiment

ATP values for the 5-FU experiment trended negatively as the dose increased (Fig 3.18). CO5-1 ATP values slightly fell at 30µM, a 8.77% ($\pm 12.2\%$) reduction, and

maintained these values through 75 μ M 5-FU (Fig 3.19). At the 100 μ M concentration ATP values began their descent but did not fall below 50% of control until 500 μ M 5-FU. At maximum concentration there was a recorded 64.8% (\pm 13.8%) reduction from baseline, and significant difference was present at concentrations of 100 μ M and greater. PMP 501-1 ATP values fluctuated within 6% of baseline through 75 μ M 5-FU (Fig 3.20). At 100 μ M ATP values fell 11.3% (\pm 15.4%), and these values were effectively maintained through 300 μ M. 5-FU. PMP 501-1 had a 36% (\pm 19.3%) reduction in ATP values from the control by 500 μ M, but there was no significance present within this interaction. ABX 023-1 ATP values consistently decreased throughout the 5-FU experiment (Fig 3.21); however, these values did not fall below 50% of control until 500 μ M. At maximum concentration, a significant reduction (p <0.0001) of 72.5% (\pm 11.4%) from the control was observed. PMP 457-2 ATP values fluctuated from baseline through 100 μ M 5-FU, with a maximum increase of 8.68% (\pm 4.89%) at 75 μ M (Fig 3.22). PMP 457-2 at maximum concentration had a significant reduction (p <0.0001) of 47.1% (\pm 20.3%) from control. ATP values for CO9-1 trended negatively through the 5-FU dose curve (Fig 3.23). These values fell below 50% of control at 300 μ M and 500 μ M, 50.7% (\pm 14.4%) and 62.0% (\pm 13.3%) respectively, and significant reductions were present at both concentrations.

3.5 Oxaliplatin Experiment

Four of the five tested cancers had a negative trend for ATP values as the concentration of Oxp increased, and only CO9-1 ATP values were in excess of baseline values (Fig 3.24). PMP 457-2 average ATP values never fell below 50% of control (Fig 3.25). The lowest recorded average ATP values occurred at 60 μ M, a 43.8% (\pm 8.29%)

reduction, and 80 μ M, a 43.8% (\pm 7.57%) reduction. Significant differences were observed at each tested concentration. CO5-1 values fell below 50% of control at both 100 μ M and 120 μ M, and by 120 μ M Oxp had a 66.7% (\pm 13.5%) reduction (Fig 3.26). Significant differences were also present at each tested Oxp concentration. CO9-1 ATP values only fell below control at 40 μ M, measured as a 20.8% (\pm 11.1%) reduction ($p=0.0232$) (Fig 3.27). At 100 μ M Oxp, ATP values were the largest in the experiment with a 11.7% (\pm 20%) increase from control. It is important to note the large variance observed in the data for CO9-1. As the concentration of Oxp increased in this experiment, the overall range of measured ATP values also increased. ABX 023-1 had significant difference present at every concentration of Oxp, and ATP values fell below 50% of control at concentrations of 80 μ M and greater (Fig 3.28). At both 100 μ M and 120 μ M the ATP values were in excess of a 70% reduction from control, 72.6% (\pm 6.26%) and 78.8% (\pm 5.53%) respectively. Significant difference was present ($p<0.0001$) for each concentration point for PMP 501-1, however at no point were average ATP values below 50% of control (Fig 3.29). At maximum concentration, PMP 501-1 ATP values were measured as a 49.3% (\pm 8.55%) reduction from control.

3.6 Irinotecan Experiment

Three of the five tested cancers had average ATP values measured in excess of control for the entirety of this experiment (Fig 3.30). PMP 501-1 ATP values consistently increased until 80 μ M which was the maximum growth observed in this experiment as a 73.6% (\pm 14.2%) increase from control (Fig 3.31). At maximum concentration ATP values were at their lowest point for this cancer, at a 38% (\pm 22.2%) increase from control. Significant differences were observed at concentrations of 80 μ M and below.

ABX 023-1 ATP values were in excess of control at concentrations between 40 μ M and 80 μ M however, peak ATP values were observed at 60 μ M with a 15% (\pm 11.9%) increase (Fig 3.32). Average ATP values began to decrease again at 80 μ M, and by 100 μ M had reduced by 65.8% (\pm 16.8%) as compared to the control. A significant difference was also only present at the maximum concentration of 100 μ M Irinotecan. CO9-1 had the largest measured growth in this experiment eclipsing a twofold increase in average ATP values at both 60 μ M and 80 μ M Irinotecan (Fig 3.33). Average ATP values continuously increased from control to 80 μ M Irinotecan where peak growth was observed as a 114% (\pm 28.7%) increase. ATP values begin to reduce again by 100 μ M, but still were a 93% (\pm 36.2%) increase from control. Differences were significant at each concentration point in this experiment. CO5-1 average ATP values consistently increased until 60 μ M a 28.2% (\pm 8.27%) increase from control (Fig 3.34). ATP values were effectively maintained through 80 μ M before falling below control at 100 μ M, a 30.6% (\pm 16.4%) reduction from control. Significant reductions were observed at concentrations between 40 μ M and 80 μ M Irinotecan. PMP 457-2 recorded average ATP values were in excess of control for the entirety of this experiment (Fig 3.35). These values fluctuated until 60 μ M where peak growth was observed as a 37.8% (\pm 12.3%) increase from control. Beginning at 80 μ M there is a reduction of ATP values, before falling to the smallest growth recorded at 100 μ M Irinotecan as a 7.38% (\pm 17.8%) increase from control. Significant differences were only observed at the 60 μ M and 80 μ M concentrations.

3.7 Combination Experiment

ATP values for the combination experiment were in excess of a 30% reduction in control values (Fig 3.36). PMP 501-1 values fell by 35.4% (\pm 3.77%) at 40 μ M Irinotecan

(Fig 3.37). These ATP values fluctuated within 10% as the concentration of Irinotecan increased, and by the maximum Irinotecan concentration fell 45.0% ($\pm 7.55\%$) as compared to the control. Significant differences were observed at each concentration point. CO5-1 average ATP values fell below 50% of control at concentrations of 80 μ M and 100 μ M Irinotecan, with a 79.2% ($\pm 4.98\%$) reduction from control at 100 μ M (Fig 3.38). Significant differences were obtained at each concentration point. CO9-1 initial ATP values dropped 46.2% ($\pm 5.63\%$) at 40 μ M Irinotecan, and the average values fluctuated within 6% for each of the subsequent concentrations (Fig 3.39). Peak growth was observed at 80 μ M Irinotecan as a 40.8% ($\pm 4.22\%$). Significance was present at each concentration point as well. PMP 457-2 ATP values consistently decreased as the Irinotecan concentration increased (Fig 3.40). Initially at 40 μ M there was a 40.0% ($\pm 2.11\%$) reduction from control, and by 100 μ M ATP values had further declined to 64.6% ($\pm 3.13\%$) decrease. Significance was also present at each concentration point for this interaction. ABX 023-1 values fell by 44.6% ($\pm 7.5\%$) at the 40 μ M Irinotecan concentration, and fluctuated within 6% as the concentration increased (Fig 3.41). ATP values by 100 μ M had reduced from the control well by 49.4% ($\pm 10.8\%$). Significant difference was observed at each concentration point.

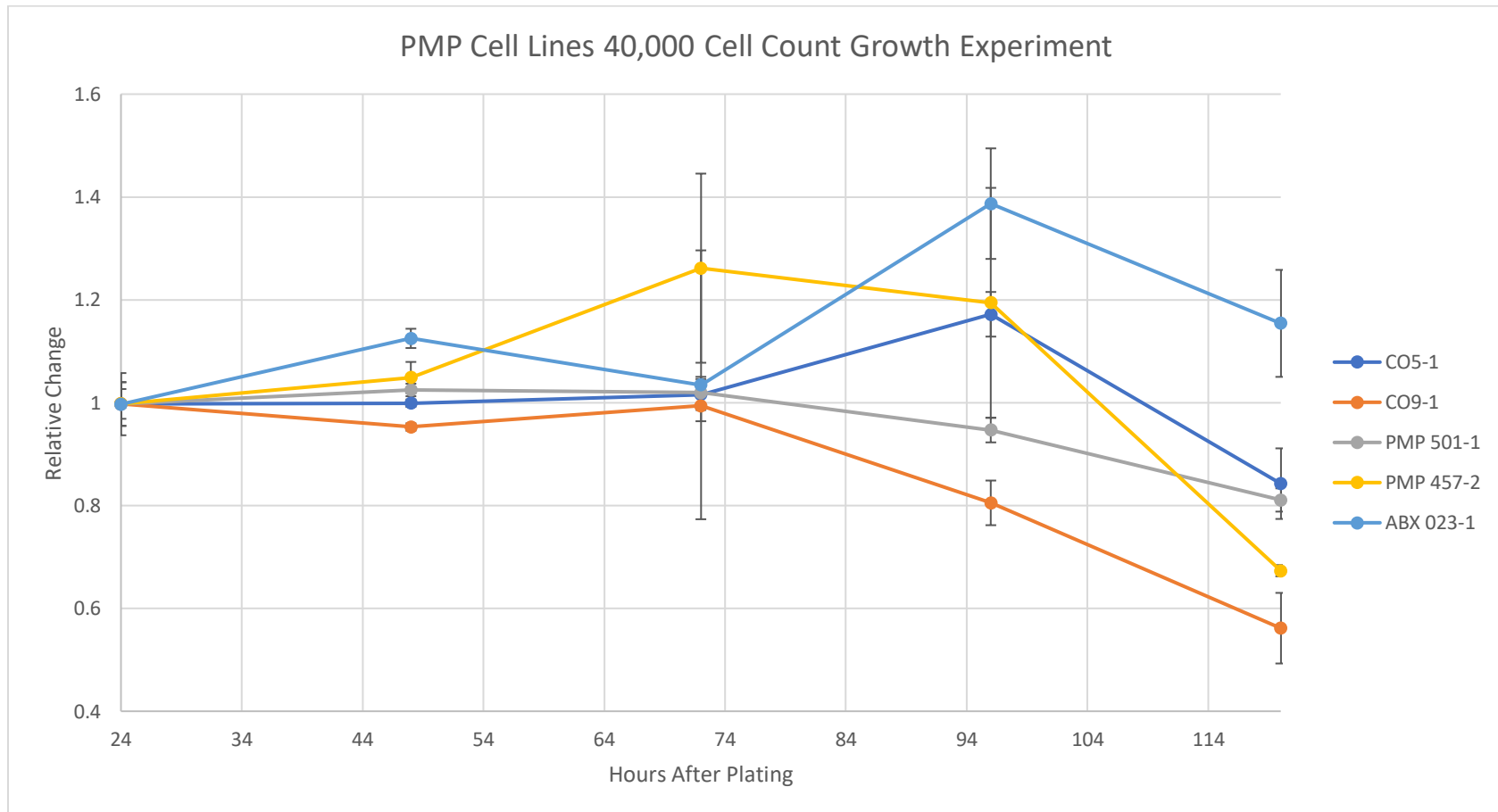


Figure 3.1 PMP cell line growth experiment. 40,000 cell count.

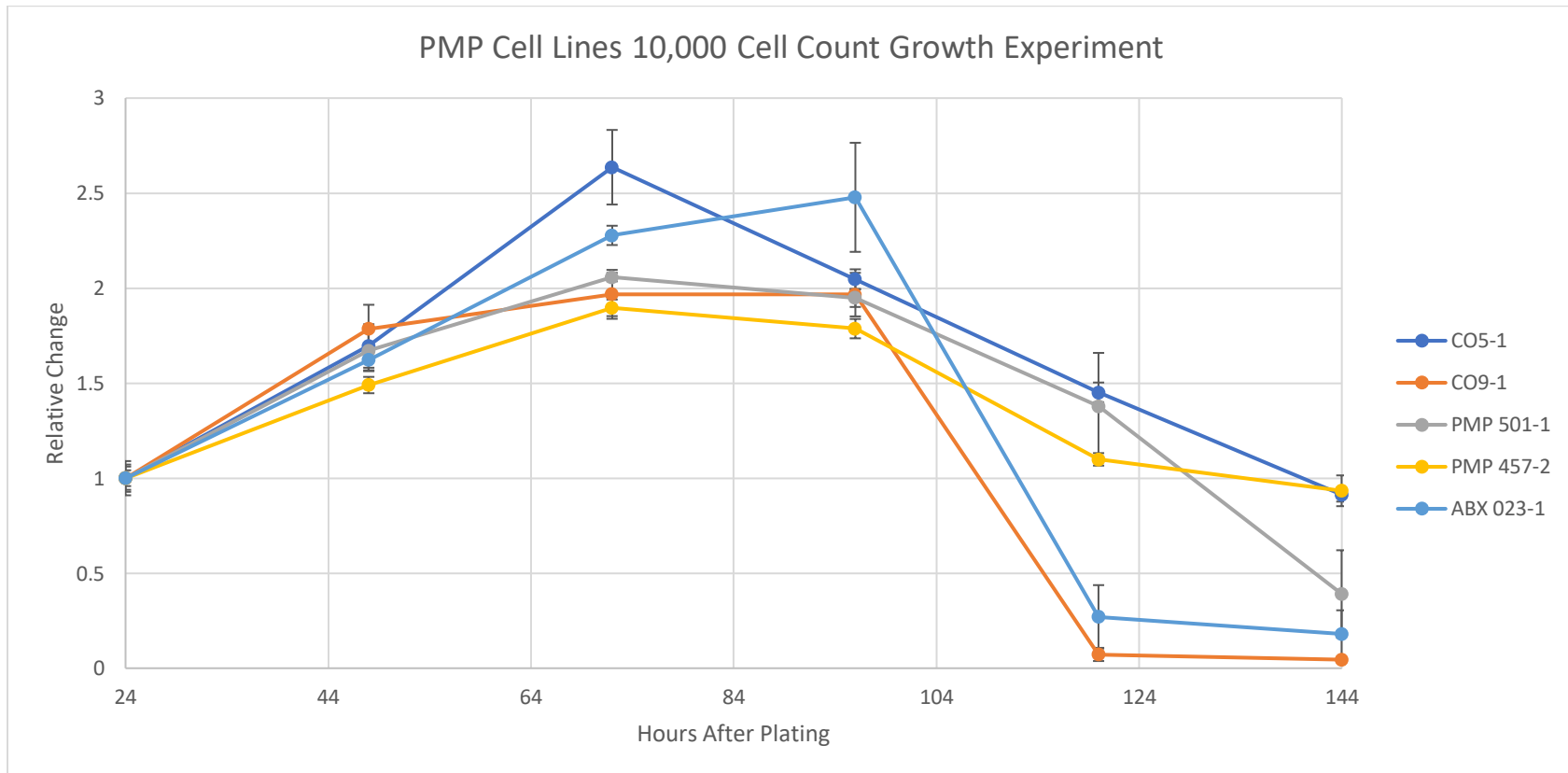


Figure 3.2 PMP cell line growth experiment. 10,000 cell count.

ABX 023-1 10000 Cell Growth Experiment

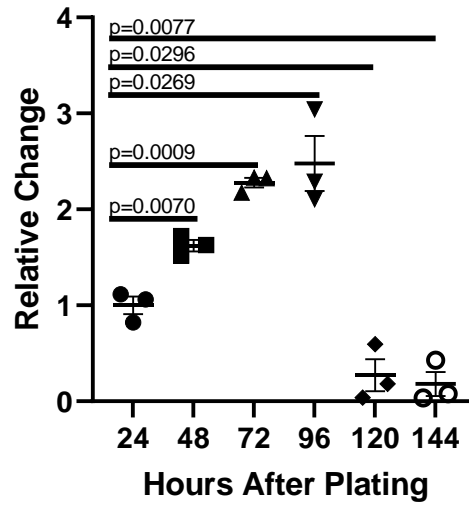


Figure 3.3 ABX 023-1 average ATP values. 10000 cell count growth trial.

PMP 457-2 10000 Cell Growth Experiment

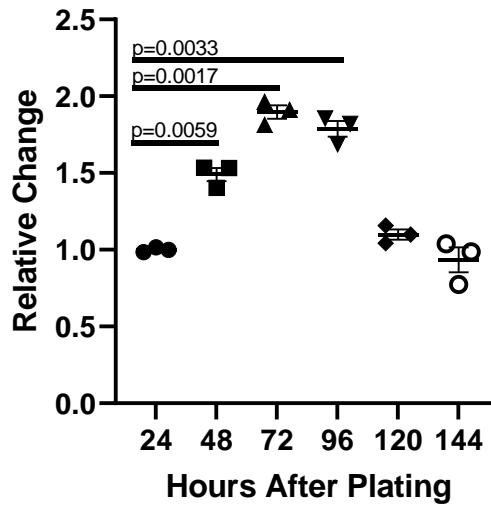


Figure 3.4 PMP 457-2 average ATP values. 10000 cell count growth trial

CO9-1 10000 Cell Growth Experiment

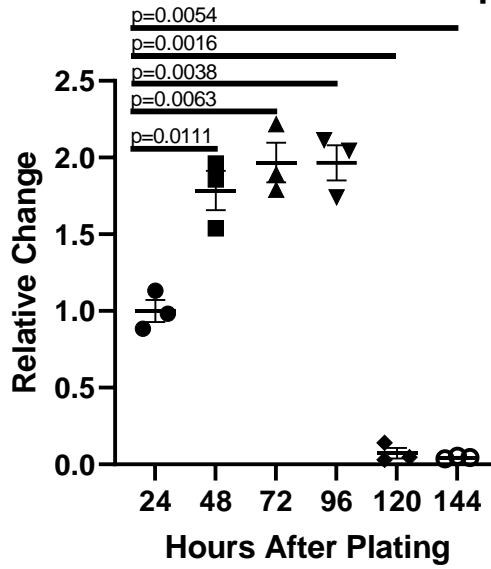


Figure 3.5 CO9-1 average ATP values. 10000 cell count growth trial.

CO5-1 10000 Cell Growth Experiment

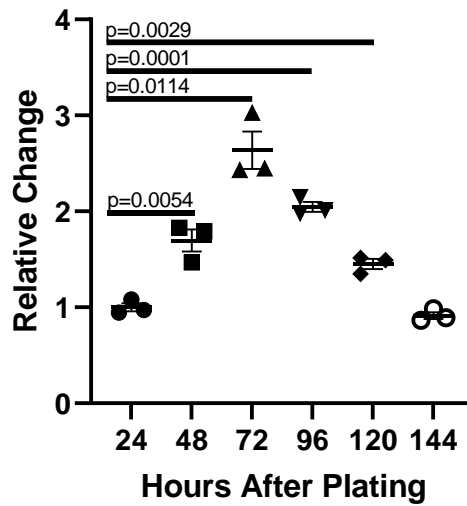


Figure 3.6 CO5-1 average ATP values. 10000 cell count growth trial.

PMP 501-1 10000 Cell Growth Experiment

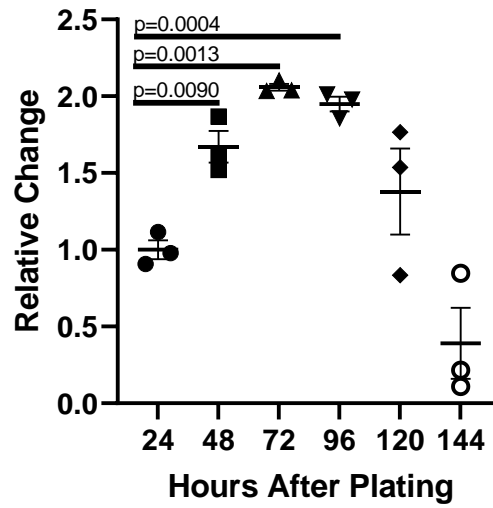


Figure 3.7 PMP 501-1 average ATP values. 10000 cell count growth trial.

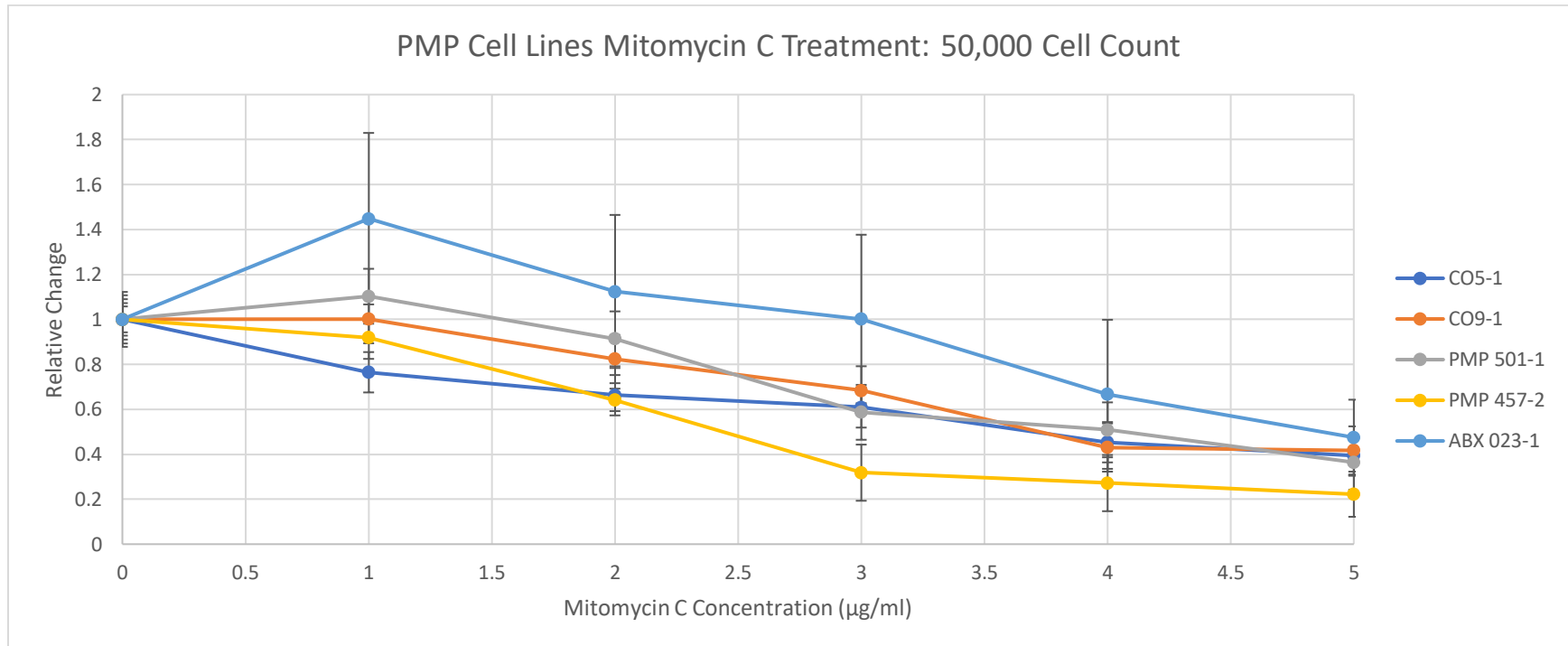


Figure 3.8 PMP Cell lines treated by MMC therapy at 50,000 cell count.

PMP 457-2 ATP Values, 50000 Cell Count / MMC

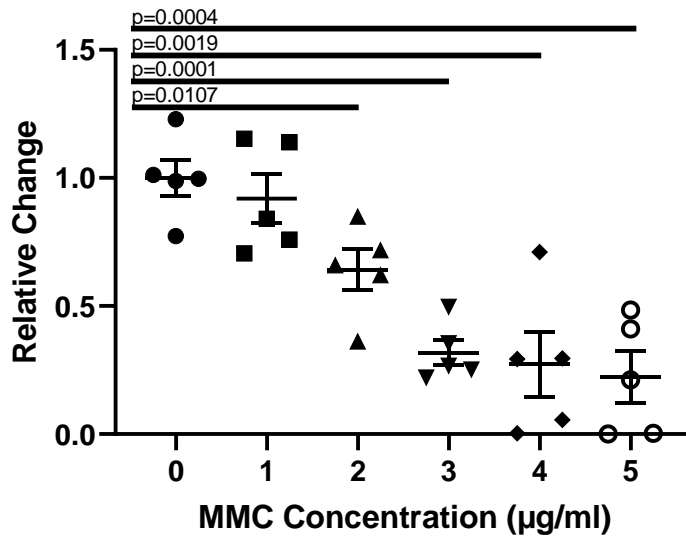


Figure 3.9 PMP 457-2 ATP values as treated by MMC 50,000 cell count

PMP 501-1 ATP Values, 50000 Cell Count / MMC

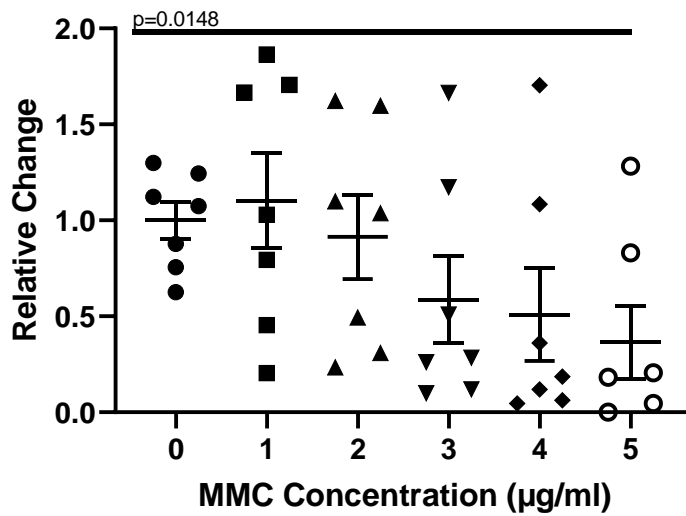


Figure 3.10 PMP 501-1 ATP values as treated by MMC 50,000 cell count

ABX 023-1 ATP Values, 50000 Cell Count / MMC

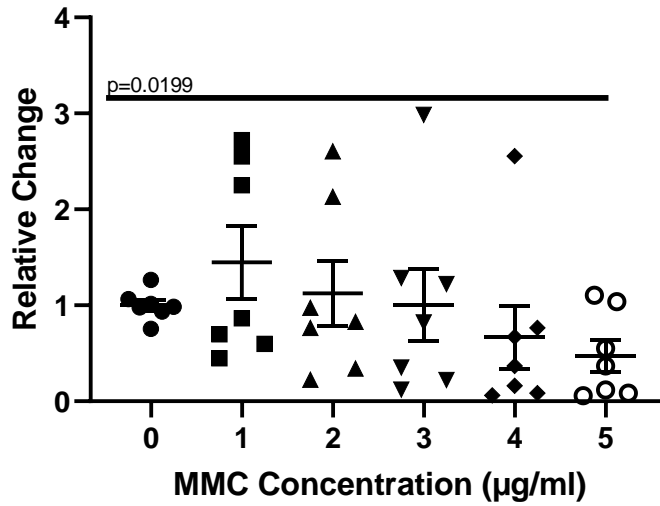


Figure 3.11 ABX 023-1 ATP values as treated by MMC 50,000 cell count

CO9-1 ATP Values, 50000 Cell Count / MMC

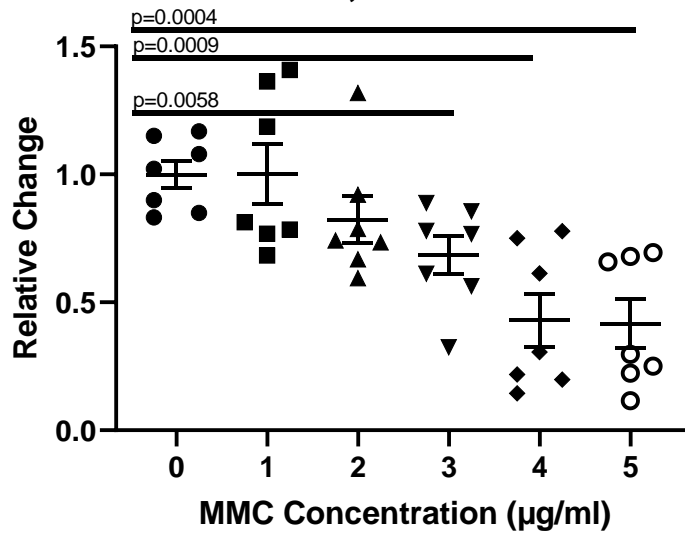


Figure 3.12 CO9-1 ATP values as treated by MMC 50,000 cell count

CO5-1 ATP Values, 50000 Cell Count / MMC

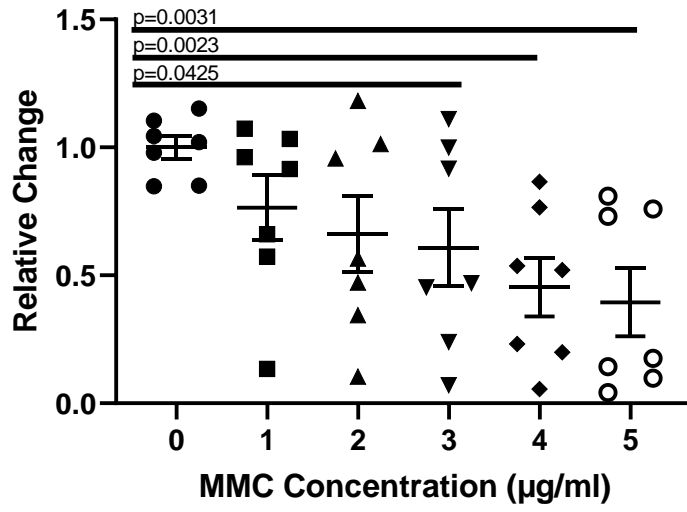


Figure 3.13 CO5-1 ATP values as treated by MMC 50,000 cell count.

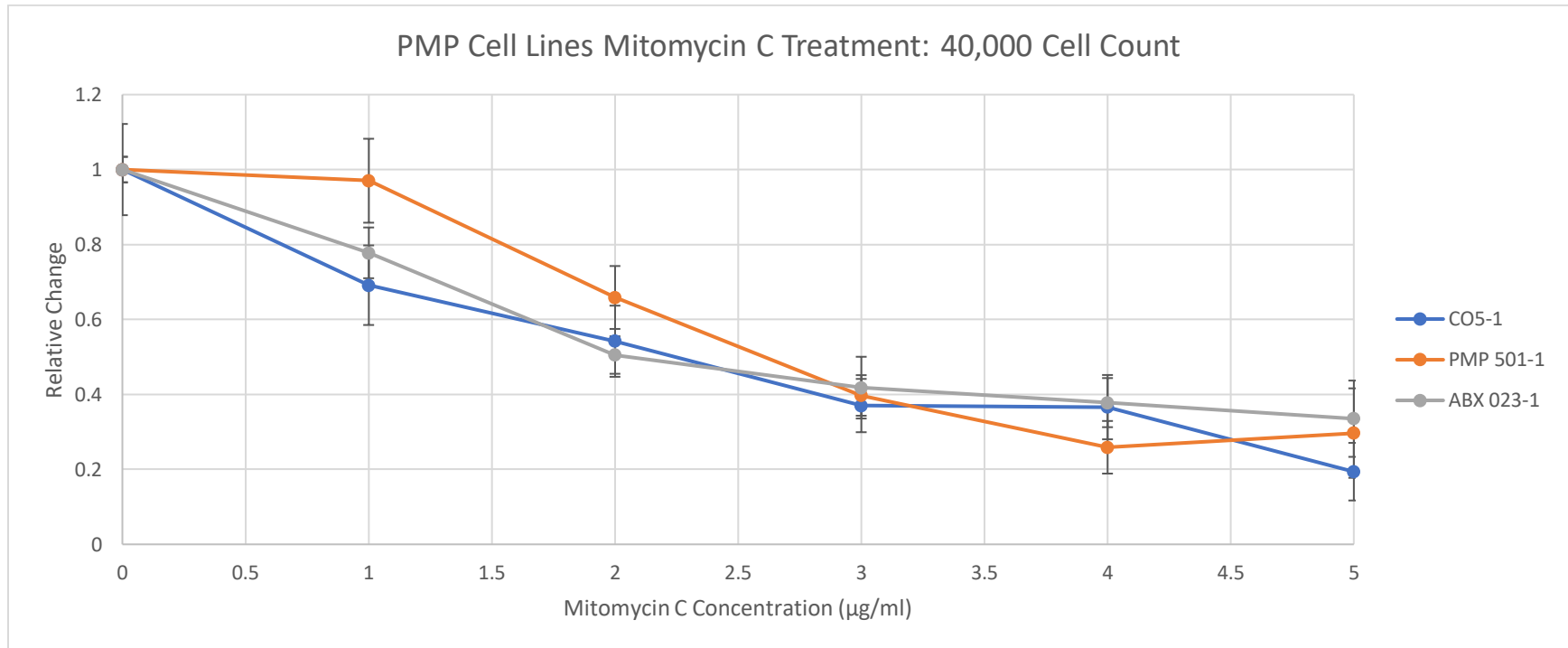


Figure 3.14 PMP cell lines treated by MMC therapy. 40,000 cell count trial

ABX 023-1 ATP Values, 40000 Cell Count / MMC

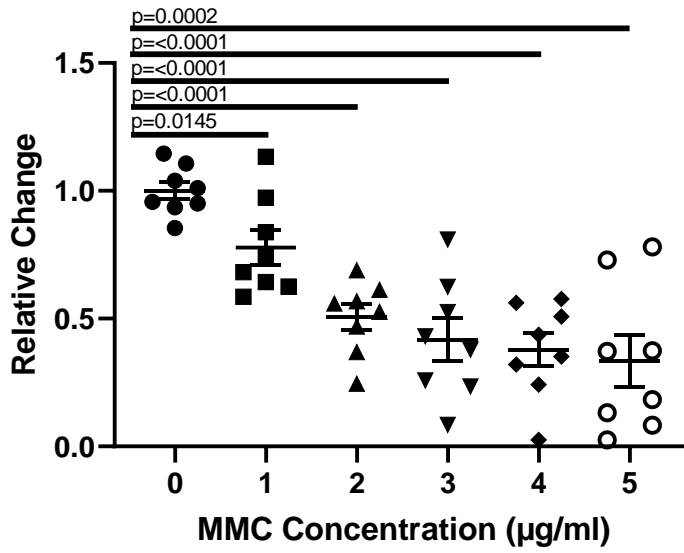


Figure 3.15 ABX 023-1 ATP values as treated by MMC 40,000 cell trial

PMP 501-1 ATP Values, 40000 Cell Count / MMC

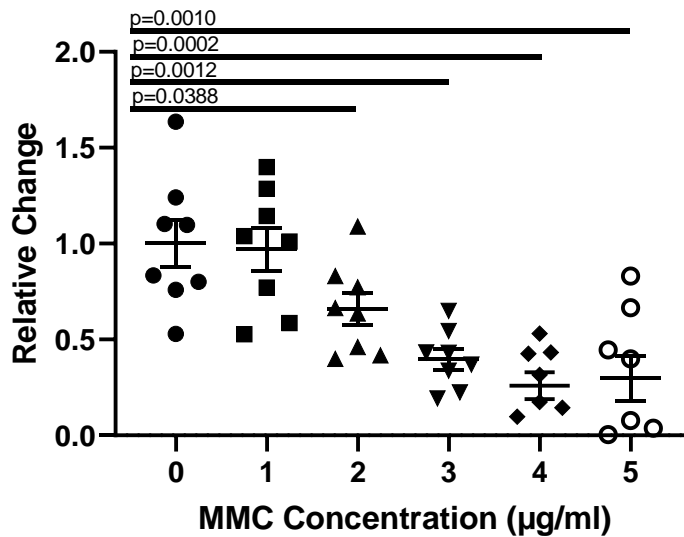


Figure 3.16 PMP 501-1 ATP values as treated by MMC 40000 cell trial

CO5-1 ATP Values, 40000 Cell Count / MMC

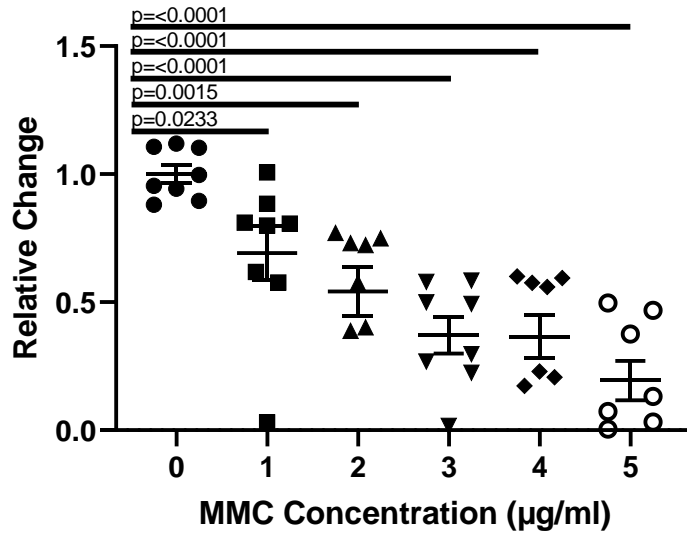


Figure 3.17 CO5-1 ATP values as treated by MMC 40000 cell trial.

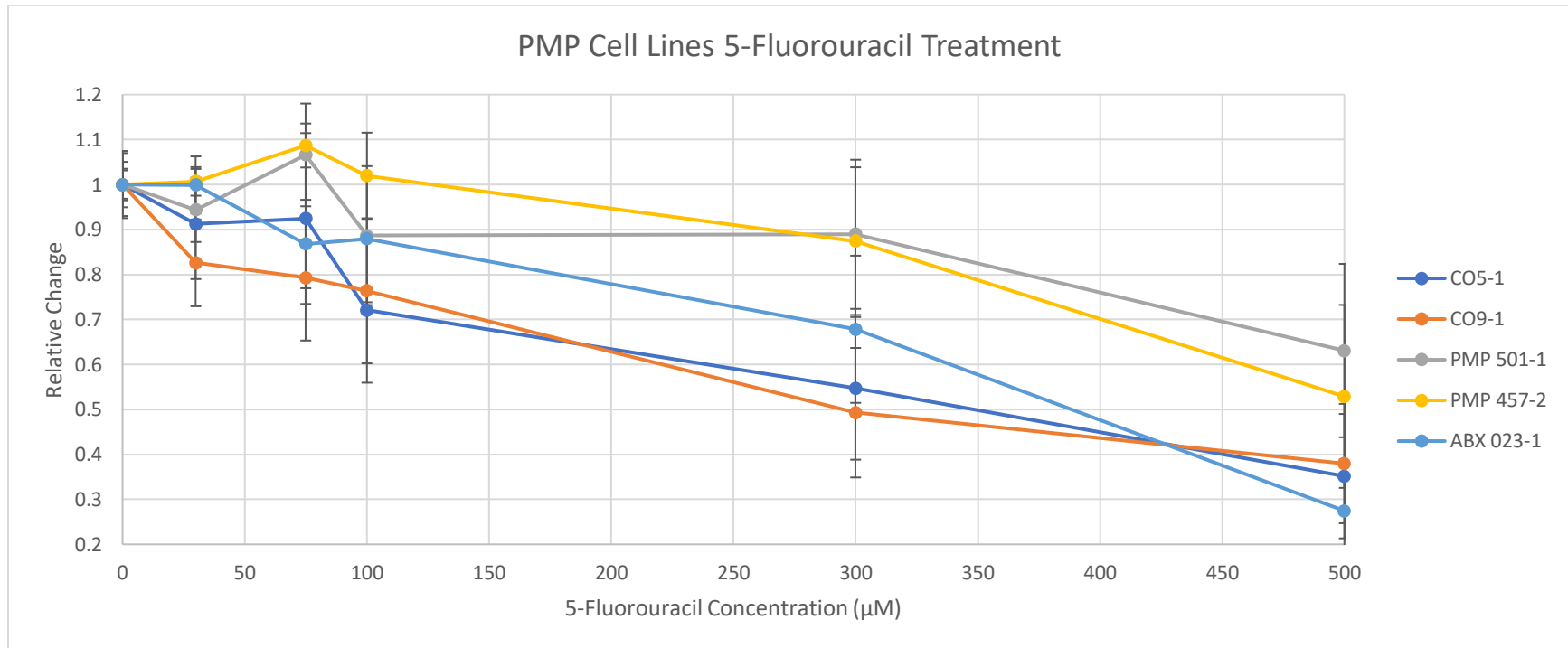


Figure 3.18 PMP Cell lines treated with 5-FU therapy

CO5-1 ATP Values / 5-Fluorouracil

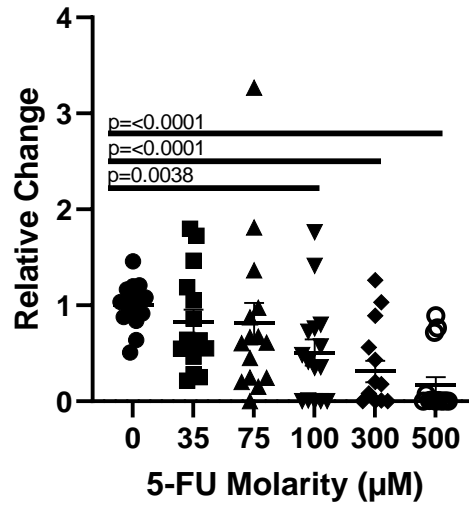


Figure 3.19 CO5-1 ATP values as treated by 5-FU

PMP 501-1 ATP Values / 5-FU

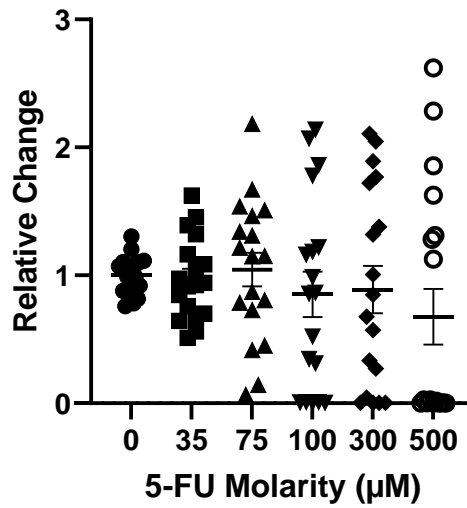


Figure 3.20 PMP 501-1 ATP values as treated by 5-FU

ABX 023-1 ATP Values / 5-Fluorouracil

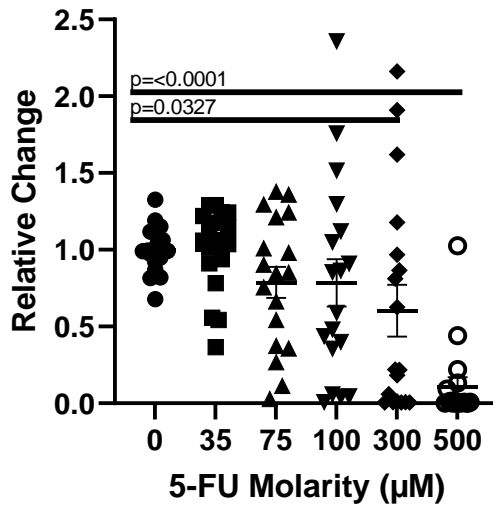


Figure 3.21 ABX 023-1 ATP values as treated by 5-FU

PMP 457-2 ATP Values / 5-Fluorouracil

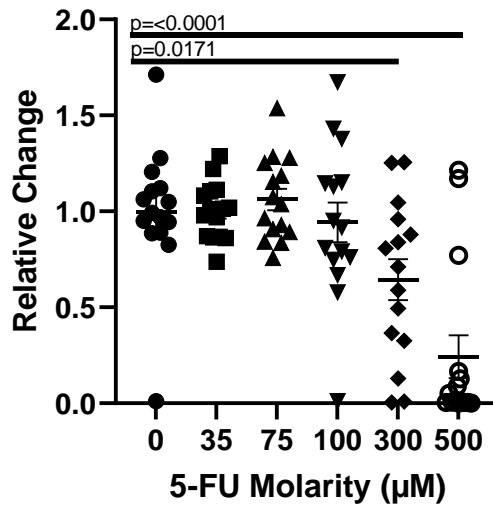


Figure 3.22 PMP 457-2 ATP values as treated by 5-FU

CO9-1 ATP Values / 5-Fluorouracil

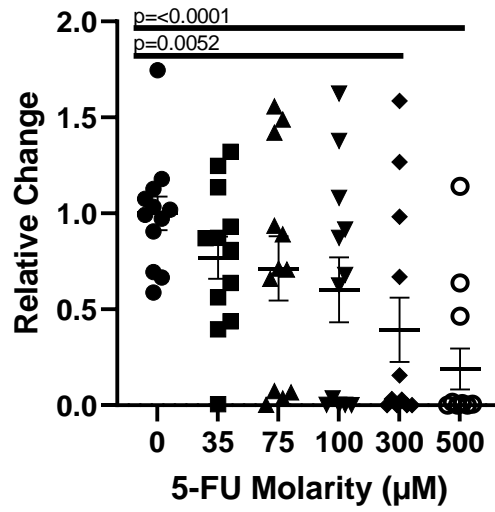


Figure 3.23 CO9-1 ATP values as treated by 5-FU.

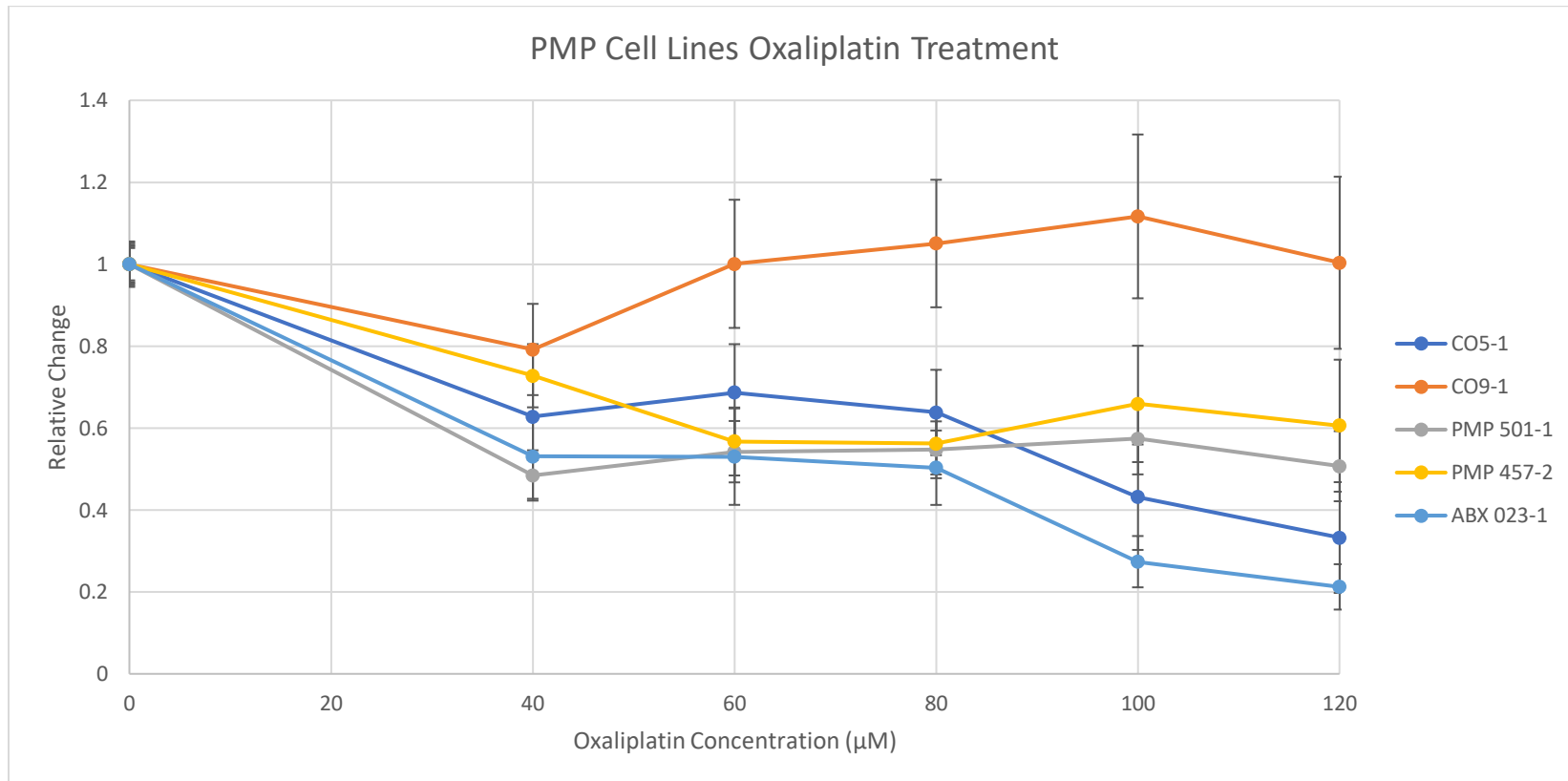


Figure 3.24 PMP cell lines treated by Oxp therapy.

PMP 457-2 ATP Values / Oxaliplatin

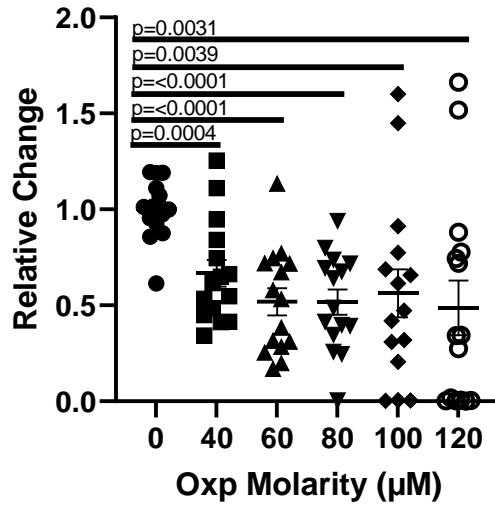


Figure 3.25 PMP 457-2 ATP values as treated with Oxp

CO5-1 ATP Values / Oxaliplatin

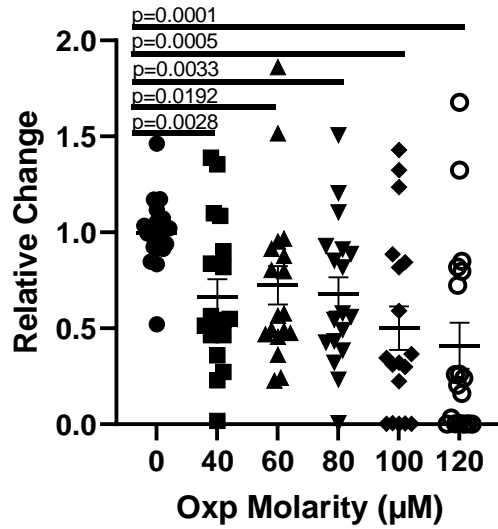


Figure 3.26 CO5-1 ATP values as treated with Oxp

CO9-1 ATP Values / Oxaliplatin

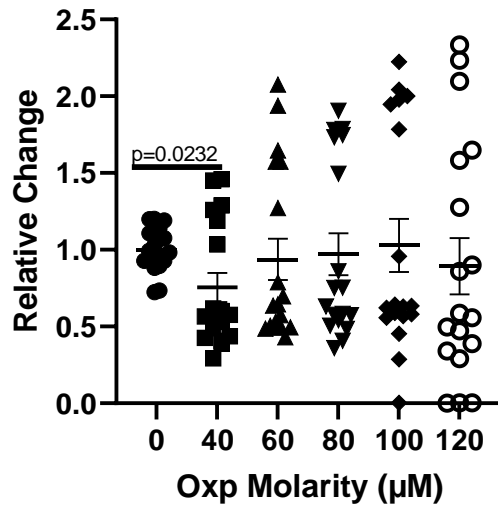


Figure 3.27 CO9-1 ATP values as treated with Oxp

ABX 023-1 ATP Values / Oxaliplatin

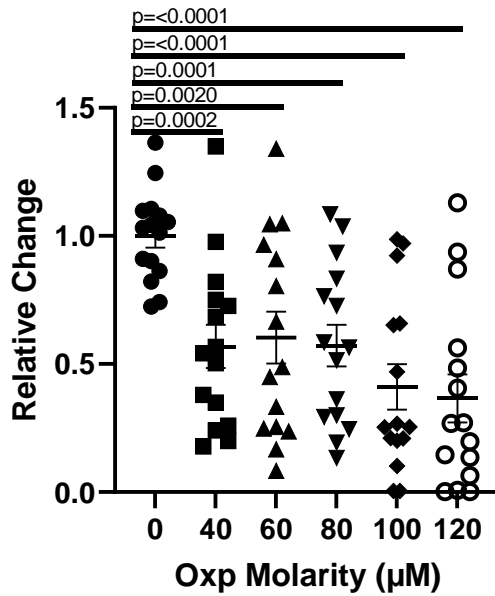


Figure 3.28 ABX 023-1 ATP values as treated with Oxp

PMP 501-1 ATP Values / Oxaliplatin

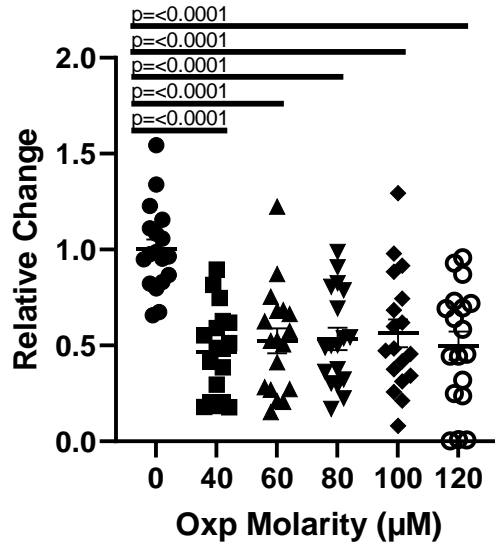


Figure 3.29 PMP 501-1 ATP values as treated with Oxp.

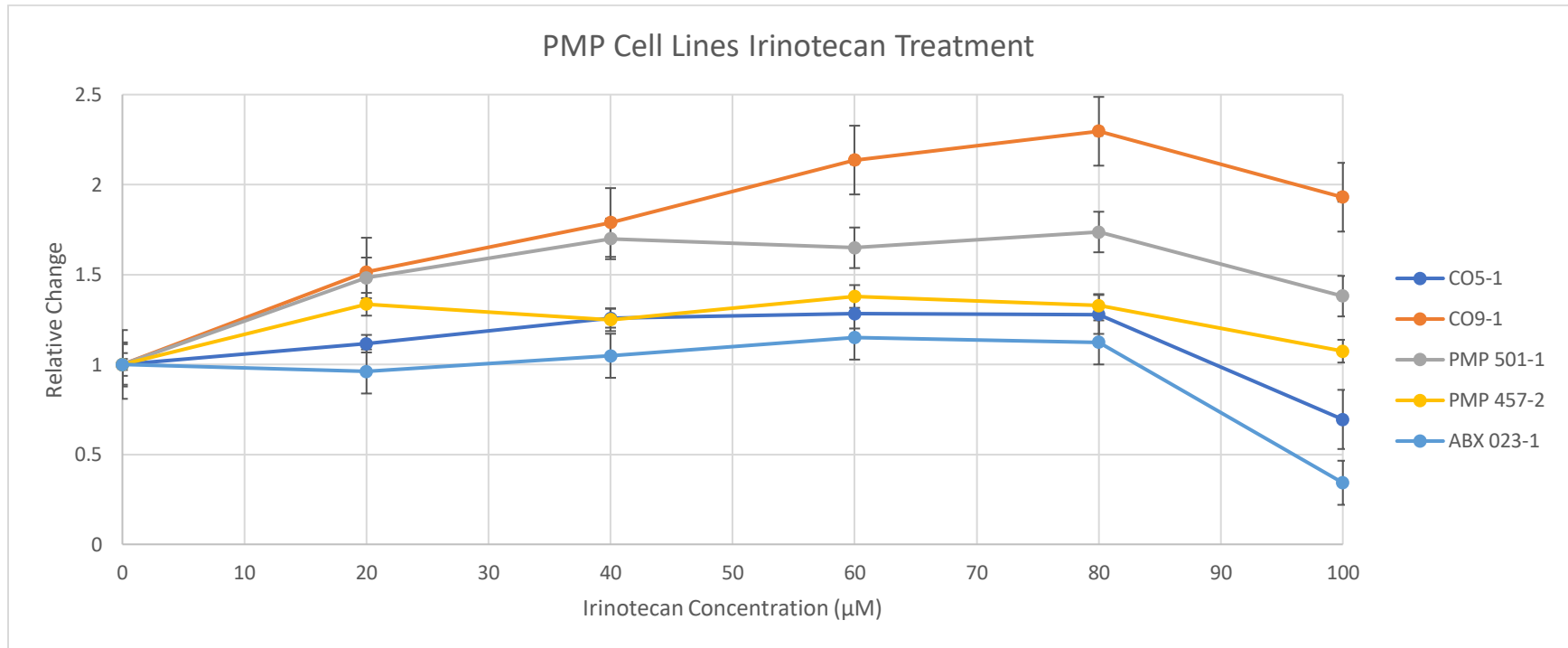


Figure 3.30 PMP cell lines treated by Irinotecan therapy

PMP 501-1 ATP Values / Irinotecan

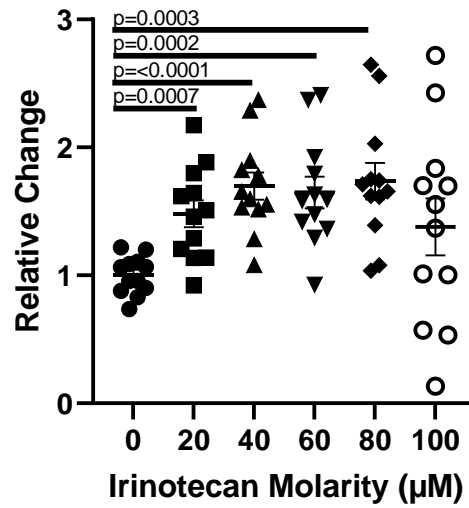


Figure 3.31 PMP 501-1 ATP values as treated with Irinotecan

ABX 023-1 ATP Values / Irinotecan

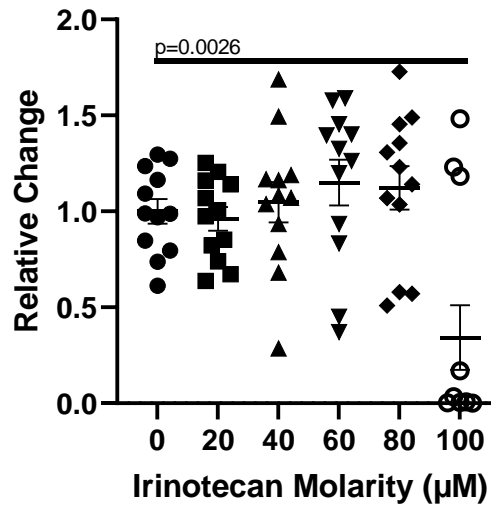


Figure 3.32 ABX 023-1 ATP values as treated with Irinotecan

CO9-1 ATP Values / Irinotecan

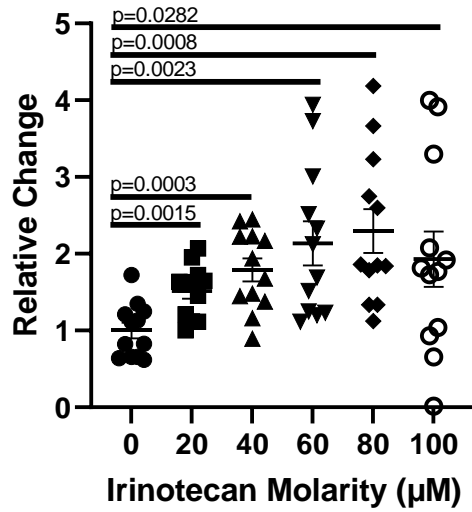


Figure 3.33 CO9-1 ATP values as treated with Irinotecan

CO5-1 ATP Values / Irinotecan

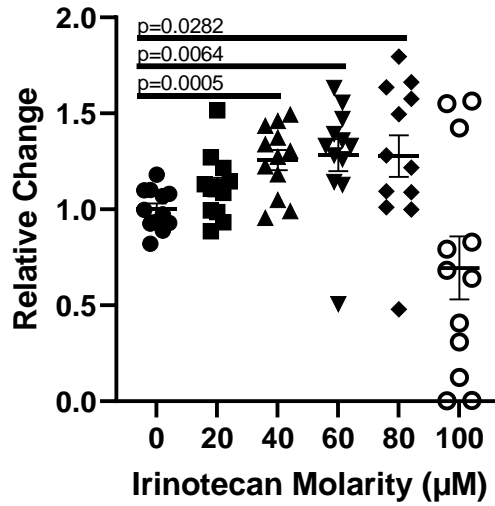


Figure 3.34 CO5-1 ATP values as treated with Irinotecan

PMP 457-2 ATP Values / Irinotecan

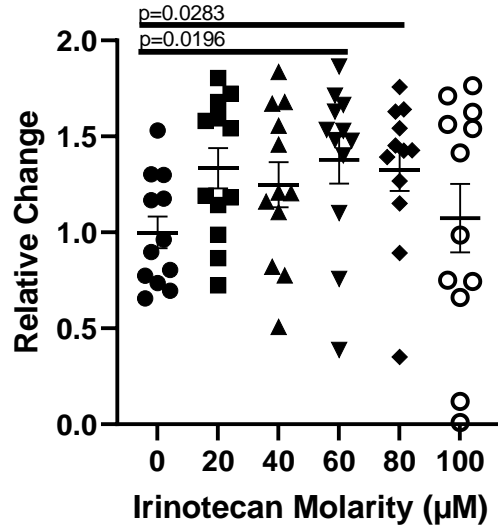


Figure 3.35 PMP 457-2 ATP values as treated with Irinotecan.

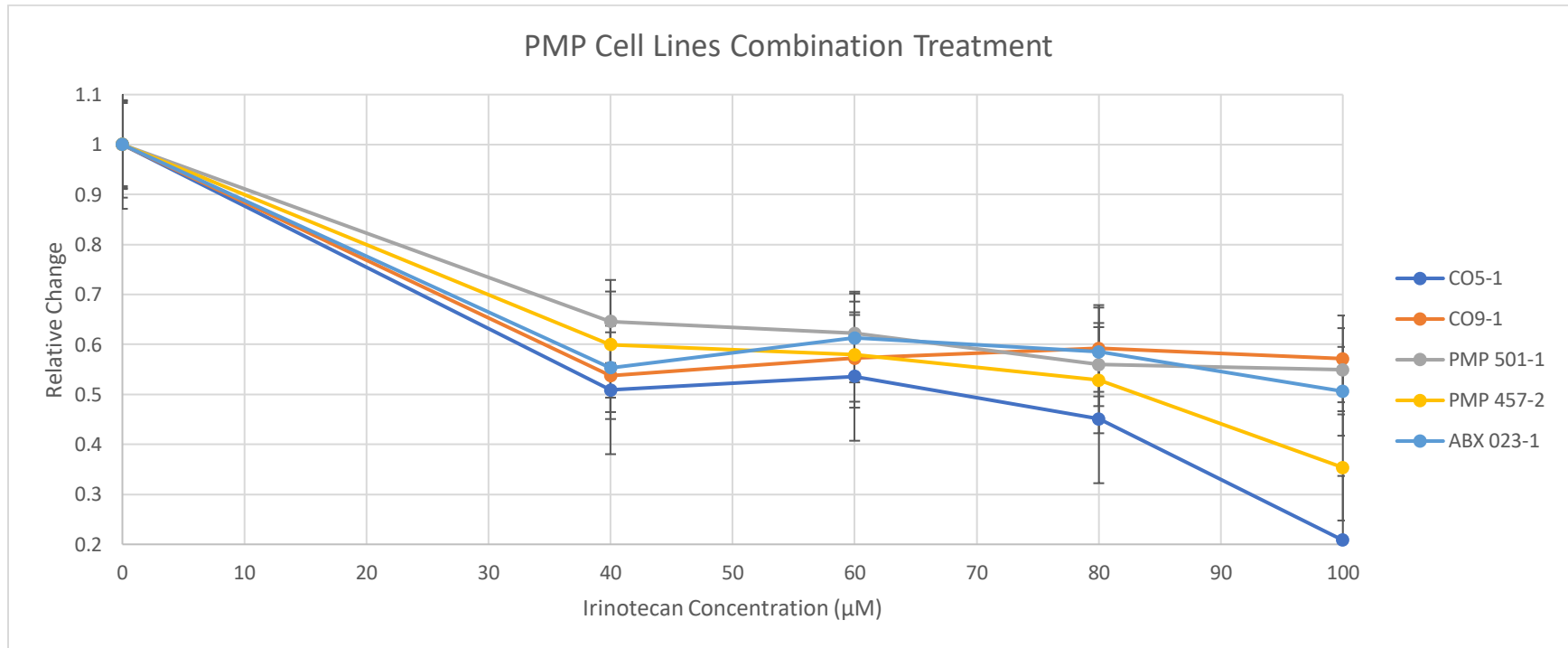


Figure 3.36 PMP cell lines treated by 5-FU/Irinotecan combination therapy

PMP 501-1 ATP Values / Combination Therapy

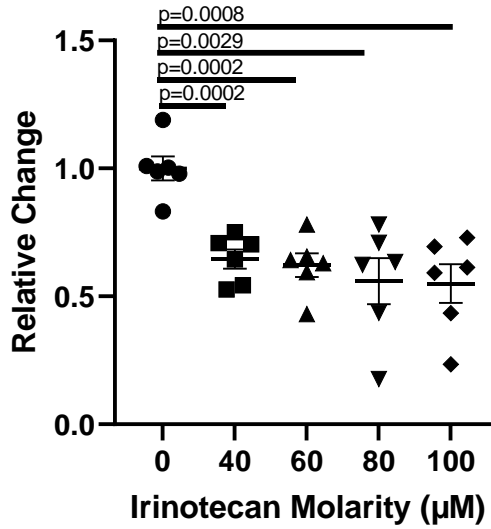


Figure 3.37 PMP 501-1 ATP values as treated by 5-FU/Irinotecan combination

CO5-1 ATP Values / Combination Therapy

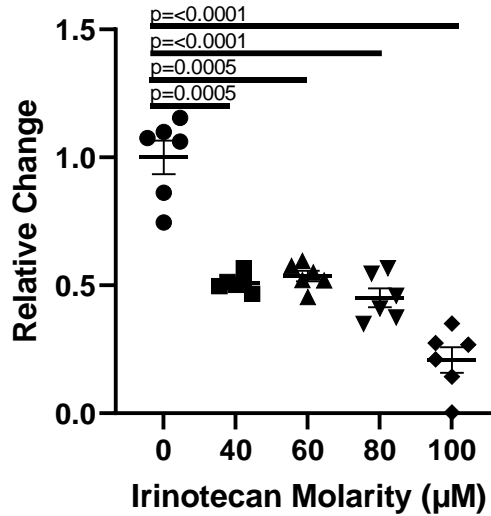


Figure 3.38 CO5-1 ATP values as treated by 5-FU/Irinotecan combination

CO9-1 ATP Values / Combination Therapy

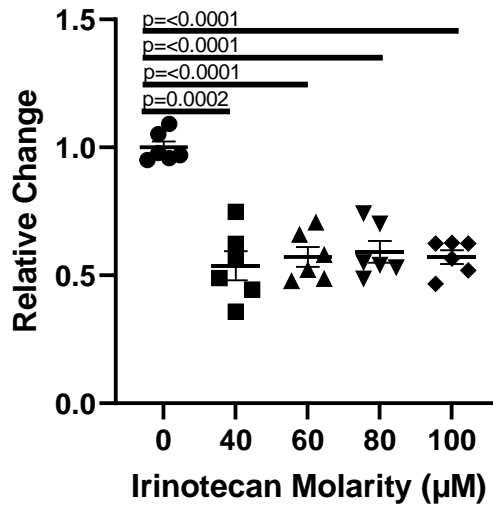


Figure 3.39 CO9-1 ATP values as treated by 5-FU/Irinotecan combination

PMP 457-2 ATP Values / Combination Therapy

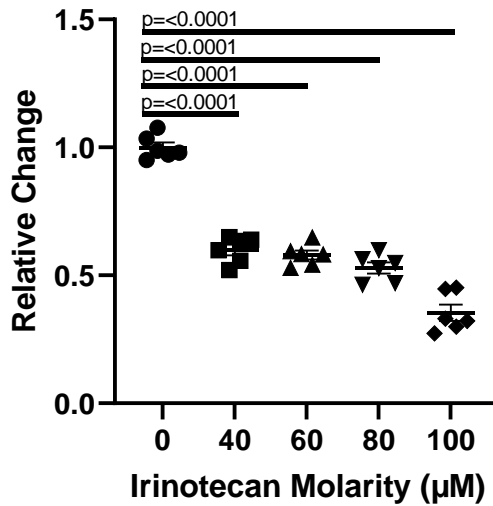


Figure 3.40 PMP 457-2 ATP values as treated by 5-FU/Irinotecan combination

ABX 023-1 ATP Values / Combination Therapy

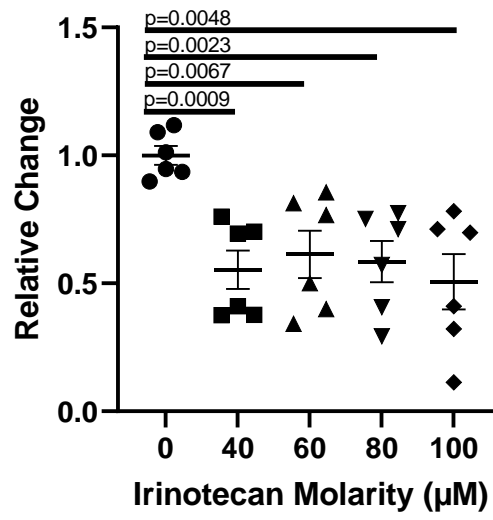


Figure 3.41 ABX 023-1 ATP values as treated by 5-FU/Irinotecan combination.

Table 3.1 Results summary table: Cell type, doubling time, and LD50

Cell Line	Type	Doubling Time (hr)	MMC 50,000 LD50 (µg/ml)	MMC 40,000 LD50 (µg/ml)	5-FU LD50 (µM)	Oxaliplatin LD50 (µM)	Irinotecan LD50 (µM)	Combination Treatment (µM)
CO5-1	Colon: sigmoid mucinous adenocarcinoma	54.5	3.78	2.68*	349.4*	89.7	451.4	61.71
CO9-1	Colon: cecum mucinous adenocarcinoma moderately differentiated	68.6	4.16		363.5*	High	High	223.6
PMP 501-1	DPAM, well differentiated	67.2	4.13	3.07*	738.3	100.5	High	96.3
PMP 457-2	DPAM, well differentiated	76.7	2.85*		582.8	129.2	High	75.2
ABX 023-1	PMCA-S moderate to poorly differentiated	67.3	5.61	3.02*	369.8*	68.3	210.1	90.5

CHAPTER 4

DISCUSSION

Pseudomyxoma peritonei is a rare condition, and the diagnosis is confirmed late in the development of the disease. At this time, early detection of this condition is difficult and is rarely achieved. Patients with PMP typically do not raise concerns to their physicians until they notice their abdomen growing rapidly and they experience gastrointestinal distress. In addition, PMP can be discovered by surgeons performing an unrelated procedure in the abdominal area^{44, 40}. Chemotherapy retains an integral role in the treatment of PMP, and our study aims to add additional information to an evolving field of study. However, chemotherapy alone does not force this condition into total clearance or remission. Research shows that the combination of bulk tumor removal and HIPEC as a paired treatment yield far better results than either procedure on their own⁵⁶. This bulk removal of cancerous epithelial cells, solid tumors, and mucin is related directly to the unique growth parameters of each cancer. In cases where CRS and HIPEC are unsuccessful, or when patients are inoperable, patients are subjected to more traditional systemic chemotherapy. PMP tumors are variable in cellularity and differentiation state, and the tested PMP cancers in this study reflects that. In this study, in addition to direct PMP cancers, mucinous colorectal cancers that have invaded the peritoneal cavity are also included. In addition to providing novel dose response curves to untested variants of PMP cancer, we explored the growth rates of each cancer in an

attempt to categorize the rate of proliferation and provide distinct evidence to chemotherapy sensitivity.

4.1 Growth Experiments

The chemotherapies utilized in this study encourage apoptosis of cells as they progress through the cell cycle with one exception; MMC is a non-cell cycle phase specific chemotherapy. The growth rates of the cancers that were tested can give us a glimpse into the rate of proliferation, and when that weakness can be exploited by therapy. These cancers were subjected to two growth experiments through the course of this study. Each growth experiment was initially seeded in 96 well microplates with differing cell counts: 40,000 and 10,000 cells per well. 10,000 cell doubling rates for each PMP cell line were calculated and are summarized in Table 3.1. Doubling rates for the 40,000 cell experiment could not be calculated due to the lack of exponential growth observed through the experiment. The 40,000 cell experiment initial raw ATP values were roughly 5 times larger than ATP values for the 10,000 cell experiment. This is relevant for discussion because 40,000 cells were the baseline for each chemotherapy experiment. The observed ATP values at 40,000 cells per well are more indicative of a solid tumor than at any point in the 10,000 cell experiment. The 40,000 cell experiment also shows limited proliferation across 120 hours. It is, however, important to note that by 72 hours each cell line was able to at a minimum maintain baseline values. These results confirm that ATP reduction through the course of each chemotherapy trial was not related to natural cell death.

Doubling time was calculated for each cancer in the 10,000 cell count growth experiment. However, significant ATP reduction was observed after 96 hours for 3 out of

the 5 cancers. Total proportionality of growth or initial raw ATP values show no correlation with this ATP reduction. It is theorized that a number of factors influenced the reduction of ATP values in the 10,000 cell growth experiment. Each cancer which experienced this large ATP reduction were uniquely affected by medium chemistry. Growth medium was unaltered through the course of experimentation to prevent disruption of growth and unintentional cell removal. This seemed to not significantly impact growth through 72 hours for the tested PMP cell lines, but later in the trial 3 of the 5 cell lines showed significant reductions in ATP values. It is possible that medium toxicity greatly affected cell health as the trial progressed. Toxic byproducts could have inhibited cellular growth through pH or salinity overloading. It is also possible that medium nutrition was exhausted by the 96-hour mark, and the lack of available nutrients impacted cellular growth and survival of the cancer cells post 96 hours. Cancers such as PMP 457-2 and CO5-1 seem uniquely resistant to toxicity and nutrient deficiency in the media. This could imply that CO5-1 and PMP 457-2 are able to sustain themselves in more toxic environments than the other cancer cell lines. Their ability to maintain ATP values through 144 hours is conducive to solid tumor development located in sparsely vascularized areas within the peritoneal cavity. These growth experiments should be replicated with the addition of daily media changes. This change in protocol would remove the inhibitory effects of medium toxicity, supply necessary cellular nutrition for continued growth, and should be compared to our study to further expand PMP cellular growth literature.

4.2 Sensitivity to Mitomycin C

MMC has been a mainstay for treatment of CRC for some time, and pharmacokinetic studies have tested clinical dose MMC therapy as both a solitary agent as well as part of a combination therapy. The Hartigh study tested 36 patients utilizing MMC as part of a multi-drug therapy. Peak plasma concentrations were within 0.4 and 3.2 $\mu\text{g/ml}$ ¹¹. MMC has been used in the past as both a solitary agent for CRC patients and as part of HIPEC utilizing fluoropyrimidine agents such as 5-FU²⁸. The results from our study show that every PMP cell line had sensitivity to MMC in the 50,000 cell trial. In this trial only one PMP cancer had a calculated LD50 in excess of the tested concentrations. ABX 023-1 (Fig 3.4) LD50 was calculated as 5.61 $\mu\text{g/ml}$, and does not fall within acceptable clinical parameters. However, when tested at the 40,000 cell count ABX 023-1 (Fig 3.8) LD50 falls to 3.02 $\mu\text{g/ml}$. This value does, in fact, fall within clinical MMC plasma concentrations. Significant reductions in ATP values for the 40,000 cell trial were observed at every MMC concentration. This also holds true for both PMP 501-1 and CO5-1. Within the 50,000 cell trial, the calculated LD50 for either of these PMP cell lines lie in excess of clinical plasma concentrations (Fig 3.3) (Fig 3.6), but both respond favorably at a smaller cell count, 3.07 $\mu\text{g/ml}$ (Fig 3.9) and 2.68 $\mu\text{g/ml}$ (Fig 3.10) respectively. The data showed that cellular density within the wells yielded dramatic differences in MMC concentrations necessary to suppress cellular proliferation. ABX 023-1 was the most affected by the reduction in the number of cells, yielding the largest differential with respect to LD50 values.

PMP 457-2 showed extreme sensitivity to MMC at 50,000 cells per well (Fig 3.2), and as such was the only PMP cancer in which the calculated LD50 fell within acceptable

clinical plasma concentrations. Significant reductions in ATP from the control were observed at concentrations of 2 µg/ml and higher. Unfortunately, PMP 457-2 was not available for testing at 40,000 cells per well and it is theorized that this cancer would follow the observed trend in this study. Additional testing at 40,000 cells per well could validate this theory, and should be explored in the future along with testing CO9-1. At 50,000 cells, CO9-1 had a calculated LD50 of 4.16 µg/ml which is higher than acceptable plasma concentrations (Fig 3.5). If CO9-1 also followed the observed trend with respect to lower cell counts, then it is possible that MMC could be used as therapy for this variant.

With 10,000 less cells per well each cancer responded very favorably to MMC, and in practice this data could be implemented with respect to treatment of solid tumors in PMP cases. Our in vitro experiments of both 50,000 and 40,000 cells per well is more reminiscent of tumor development, rather than epithelial cell strips often found suspended in mucin. Solid tumors are not uncommon in patients with PMP. CRS may remove visible tumors from the interior surfaces of the patient's peritoneal cavity, but tumors that are not visible, due to either location of the tumor or buried underneath the tissue surface, escape this procedure. MMC has a history of use as part of PMP related HIPEC, and our results show that at high cellular densities MMC is extremely effective. The sensitivity to both CO and oxygen prevents MMC from full efficacy in densely vascularized regions of the body. The relative lack of vascularization inside the peritoneal cavity minimizes oxidative stress that the agent would otherwise encounter. Additionally, lower cell densities than ones tested might respond even more dramatically. This data is promising for MMC as a solitary chemotherapy agent for 4 out of the 5 PMP cancers in this study.

CO9-1 is a prime target for additional testing with multidrug therapy utilizing MMC as one of the agents.

4.3 Sensitivity to 5-Fluorouracil

5-FU is an integral chemotherapy agent in multi-drug therapeutics such as FOLFOX and FOLFOXIRI in the treatment of PMP. However, prior to our study these variants of PMP cancers were absent of specific dose response curves relating to 5-FU as a solitary agent. 5-FU imparts anti-tumor action through inhibition of thymidylate formation, and overall inhibition of DNA and RNA synthesis leading to cellular apoptosis⁶³. Literature searches revealed a wide range of plasma concentration values that were clinically relevant for 5-FU. C_{max} for 5-FU was calculated as 6.23-55.44 μ g/ml (426.19 μ M) in the Casale study after using clinically relevant doses on patients with CRC⁵. Chemotherapy-induced toxicities are observed in patients regardless of dose extremity; however, these toxicities are typically amplified at higher doses. The tested dose concentrations were instituted based on previous cell culture trials and these concentrations fall in line with clinically relevant plasma concentrations.

Of the tested cancers, only 3 had calculated LD50s which fell within acceptable clinical plasma concentrations. CO5-1 (Fig 3.12), CO9-1 (Fig 3.16), and ABX 023-1 (Fig 3.14) responded favorably to 5-FU therapy. 5-FU attacks cells during the synthesis phase of the cell cycle, so it is surprising to see that PMP 457-2 was not uniquely impacted by this therapy. In the 40,000 cell growth experiment PMP 457-2 was observed to have the largest increase in growth within 72 hours. The other PMP cancers were recorded to show minimal comparative ATP value fluctuations during this time period. Both ABX 023-1 and CO5-1 had significantly smaller initial ATP values in the 40,000 cell growth

experiment as compared to CO9-1, but this also shows no correlation with the calculated LD50: 369.8 μM , 349.4 μM , and 363.5 μM respectively. It appears that the difference of cellular density had little impact on the efficacy of 5-FU in this experiment.

5-FU therapy could be an effective solitary agent for chemotherapeutic intervention in 3 of the 5 tested PMP cancers. The results show significant cell death at concentrations of 300 μM 5-FU and larger. However, to obtain complete, or nearly complete, cancer cell eradication would require 5-FU concentrations far in excess of safe plasma concentrations for systemic chemotherapy. The initial plating of PMP cancer cells aimed for complete confluency within the well, and this density impacted the efficiency of 5-FU with inducing apoptosis. There is historical precedence of 5-FU used as treatment for solid state tumors in CRC ⁵. This brings into focus the combined effort of fluoropyrimidine agents and other chemotherapies seen often in HIPEC interventions. 5-FU is known to have significant, at times debilitating, chemotherapy induced toxicities as outlined earlier. It is possible to reduce some of the more dangerous toxicities of 5-FU by pairing it with another CRC agent. FOLFOX, and FOLFOXIRI are shown to be extremely effective as an intervention for CRC. Hyperthermic administration has been shown to have no bearing on the efficacy of 5-FU action specifically, however the addition of numerous chemotherapy agents allows for a multi-pronged attack on PMP cancer ²⁴. Because of the lack of vascularization inherent within the peritoneal cavity, physicians are able to administer HIPEC at higher concentrations than would be used in systemic chemotherapy.

4.4 Sensitivity to Oxaliplatin

Oxaliplatin is a platinum-based chemotherapy agent used in the treatment of both CRC and PMP which, while in vivo, is transformed to active metabolites that bind to both guanine and cytosine nucleotides. This binding leads to lethal crosslinking of DNA and inhibition of nuclear functionality within the cell⁶³. Oxaliplatin is an integral part of the multidrug therapy FOLFOX, utilized as a form of HIPEC. In phase I studies, Oxaliplatin was administered to patients with various forms of cancer including CRC. A review of Oxaliplatin pharmacokinetics determined that over a 2-hour treatment, C_{max} values fell between 2.59-3.22 $\mu\text{g/ml}$ ($8\mu\text{M}$)¹⁹.

The results from our study shows that 4 of 5 PMP cell lines responded favorably to Oxp at concentrations 60 μM and greater (Fig 3.17). The only PMP cancer that lacked sensitivity to Oxp was CO9-1 (Fig 3.20), and careful analysis of the data reveals an interesting division within each concentration. An LD50 could not be calculated due to the average increase in ATP values as concentration increased. Significant difference was only present between the control well and 40 μM , with higher concentrations yielding no significant change from control. Each tested Oxp concentration shows two pools of ATP values, which grow further apart as the concentration increases in the CO9-1 experiment. The ATP values tend to congregate around 50% of control values and an increase of 50-100% compared to control. Roughly 50% of the wells showed sensitivity to Oxp, but it would be disingenuous to neglect the fact that 50% of wells showed at a minimum an inability to restrict normal cellular proliferation.

ABX 023-1 showed the most sensitivity to Oxp, with a calculated LD50 of 68.33 μM (Fig 3.21). This particular cancer showed significant ATP reduction at every tested

Oxp concentration when compared to the control well. Of course, variance within each concentration is present; however, ATP value densities do not congregate in two unique pools as seen in CO9-1. It is therefore with some confidence that our study shows sensitivity with this specific cancer and chemotherapy interaction. PMP 501-1 also showed a peculiar interaction with Oxp. Each tested Oxp concentration shows a significant reduction from the control wells, $p < 0.0001$, however average ATP values show a range of reductions from 42.6% to 51% of the control across the dose range (Fig 3.22). These ATP values show a similar density as the Oxp concentration increases, and due to the moderate sensitivity observed by the results of the study it is theorized that PMP 501-1 would yield more promising results with a combination therapy utilizing Oxp with another agent, or hyperthermic administration of the Oxp agent.

Each calculated LD50 fell in excess of acceptable clinical plasma concentrations. Dose related toxicities of Oxaliplatin limit the total dose administered to patients undergoing treatment as systemic chemotherapy. Oxp as administered in this trial as a solitary agent may not be an effective means to treat these specific PMP cancers. There is precedence of Oxp utilized as part of a multi drug therapy capitalizing on fluoropyrimidine agents such as 5-FU²⁰. Due to time limitations the specific synergy between 5-FU and Oxp was not explored in this study. In addition, with respect to HIPEC procedures, chemotherapy temperature was not varied from human body temperature in this study. HIPEC administers chemotherapy agents at 41°C, but due to the lack of standardization with HIPEC procedures this temperature can have small variations. Hyperthermic platinum-based chemotherapies are shown to have a tumor suppressive effect when utilized in HIPEC. The Helderman study shows a temperature differential of

1°C above body temperature significantly improves the effectiveness of the platinum agent. Human colorectal cells respond favorably to increased temperatures, noting a 30% reduction in cell viability at 43°C which was the highest temperature tested in the study²⁴. Our in vitro study maintained a 37°C temperature over 48 hours, and there is the possibility that short term exposure to hyperthermic Oxp, as seen in HIPEC, might yield more effective cellular death. The Helderman study has shown that platinum-based chemotherapies are exceptionally sensitive to temperature with respect to tumor suppression, yielding more apoptosis through DNA double strand breaks and increasing the rate of platinum uptake²⁴.

4.5 Sensitivity to Irinotecan and 5-Fluorouracil/Irinotecan

Irinotecan is an anti-tumor chemotherapy utilized as part of treatment protocols for advanced solid tumor CRC¹⁰. Irinotecan, and the active metabolite SN-38, impact nuclear functionality by binding to the topoisomerase I DNA complex^{5,10}. In the Chabot paper, C_{max} of Irinotecan fell within 1-10 mg/L (16nM) when utilizing a clinically recommended dose of 100 mg/m²/day. This dose was discovered in a previous phase 1 study of Irinotecan, in which the maximum tolerated dose was determined as 115 mg/m²/day when tested on patients with advanced solid tumors^{7,6}.

Irinotecan as the sole chemotherapeutic did not yield promising results (Fig 3.23). With the exception of ABX 023-1 and CO5-1, all other PMP cell lines showed no sensitivity to Irinotecan. ATP values showed an average increase as concentrations of Irinotecan increased to 100 µM, and therefore LD50 could not be calculated for 3 out of the 5 tested cancers. LD50 for ABX 023-1 was calculated as 210.1 µM, and 451.4 µM for CO5-1. Both ABX 023-1 (Fig 3.25) and CO5-1 (Fig 3.27) calculated LD50 far exceeds

clinical dose ranges utilized in literature. It was reported that in the phase I study, leukopenia severity increased as the patients were given additional Irinotecan treatment over time. Chemotherapy related toxicities were seen in 50% of patients exposed to 115 mg/m²/day ⁶. It is important to note, however, that it has been observed in previous studies that Irinotecan tends to perform better as a cytotoxic agent in vivo rather than in vitro ³¹. This study was entirely in vitro, and should be expanded on in the future to include possible testing in animal models.

As explored earlier, CRS and HIPEC is the preferred method to attack a diagnosis of PMP. HIPEC is typically a combination of multiple chemotherapies heated to 40°C and then administered to a patient perioperatively post CRS. In this study, 5-FU and Irinotecan was used cooperatively to test the combined efficacy of the drugs. No chemotherapies in this study were heated to hyperthermic temperatures as part of the established protocol, but it would be beneficial to validate the previous hyperthermic chemotherapy studies with these unique PMP derived cancers. If CRS/HIPEC failed, or if a patient is unable to successfully undergo an operative procedure, physicians utilize systemic chemotherapy.

Due to the results obtained from the initial Irinotecan experiment, it was determined that a second experiment was merited. PMP cell line data showed a lack of inhibition with the exception of CO5-1 and ABX 023-1 showing sensitivity at 100µM Irinotecan. Irinotecan and 5-FU have been used to treat colorectal cancer as sole agents, and synergistically in various combinations ⁶⁵. Dose limiting toxicities of both 5-FU and Irinotecan restrict therapy to otherwise chemotherapeutic resistant tumors, and it was feared that the cumulative effect of these combined toxicities would significantly impact

possible synergy due to their similarities. This was not observed in practice ⁶⁵. The FDA approved Irinotecan therapy for advanced state colorectal cancer in patients which failed to respond effectively to 5-FU treatment ¹⁹. A more recent study from the University of Geneva attempted to maximize the efficiency of 5-FU and Irinotecan implementation by testing various routes of administration. Their results dictate those combinations of low dose chemotherapeutic agents yielded larger growth inhibition than solitary drugs ⁶⁵. However, it is important to note the distinction between the Geneva study and this particular one. Clinical administration of 5-FU and Irinotecan typically occurs with Irinotecan as the initial treatment followed by a bolus injection of 5-FU, and this was the implementation within the Geneva study as well ⁶⁵. Because the PMP cell lines tested in our study are bereft of established dose response curves, it was decided to administer 5-FU initially followed by Irinotecan. This sequence was chosen to help to establish a more robust profile on the sensitivity of PMP derived cancers to Irinotecan. The PMP cell lines were first treated with 100 μ M 5-FU for 6 hours and then Irinotecan for the remainder of the 48 hours. 100 μ M was chosen for this combination therapy because previous experimentation shows there was, at the highest, a 27.9% reduction of ATP values compared to vehicle control. Higher concentrations of 5-FU show a marked inhibition of cellular growth eclipsing a 50% reduction of ATP values as compared to control wells. The intention of the multidrug treatment was to effectively weaken the PMP cancer cell lines with the initial treatment of 5-FU. Once the cancer cells were primed by the 5-FU the 96 well plate was treated with the same dosages of Irinotecan to once again test the sensitivity of PMP cancer cell lines to Irinotecan. The mechanism between the two cytotoxic agents have been explored previous studies, and is not discussed in this paper.

The combination therapy data shows that each PMP cancer is affected to a greater degree than simply Irinotecan as the sole agent (Fig 3.29). Because of this increased sensitivity, LD50 could be calculated for every cell line in the trial. CO9-1 was the only PMP cell line that had a LD50 higher than tested parameters (Fig 3.32), and CO5-1 (Fig 3.31) showed the most sensitivity to the combination therapy with a LD50 of 61.71 μM . However, none of the PMP cell lines fell within acceptable Irinotecan plasma concentrations with this specific administration of chemotherapies. These results could be improved in the future by subjecting the cancers to a higher concentration of 5-FU prior to Irinotecan therapy. As discussed earlier, 5-FU clinical doses correlate to peak plasma concentrations of 426.19 μM . A modest increase to 300 μM 5-FU could theoretically further improve PMP cell line responsiveness to Irinotecan therapy. In addition, the time in which these cancers are bathed in each agent could yield improved results. The Drewinko study observed that camptothecin progressively increases in cytotoxic activity the longer it is exposed to tumors¹³. Future studies should vary the time period of treatment to determine whether or not PMP derived cancers respond similarly to lymphoma cells with respect to treatment duration. In addition, a reversal of the administration sequence mimicking clinical application should be explored.

4.6 Conclusions

Mitomycin C was the most effective chemotherapy agent in this study. Of the tested chemotherapy agents only MMC was a non-cell cycle phase specific cytotoxic agent. In addition, due to MMCs selective preference for solid tumors it is unsurprising that this agent was so effective at both the 50,000 and 40,000 cell count experiments. The other tested chemotherapies are sensitive to cellular proliferation, and the lack of growth

observed at the 40,000 cell density could be responsible for the lack luster performances of both Oxp and Irinotecan. 5-FU breaks the observed trend, with the majority of PMP cell lines obtaining a calculated LD50 well within acceptable plasma ranges. 5-FU attacks cells in S phase but is commonly utilized against solid tumors. The high cell confluency within the 40,000 cell count growth experiment was an adequate analogue of advanced cancer cell proliferation, but additional in vitro and in vivo testing is recommended to validate 5-FU and the specific interaction with PMP cell lines. 5-FU is shown to have no increased apoptosis inducing effects at hyperthermic temperatures, unlike the three other tested chemotherapeutic agents^{24, 8}. It is then theorized that the temperature of both Oxp and Irinotecan impacted their efficacy on the cancer cell lines. Future experimentation could explore clinical durations of agent therapy at hyperthermic temperatures, and this may further improve anti-cancer action on PMP derived cancers.

CO5-1 was observed to be the most sensitive cell line in this study. Calculated LD50s were the lowest in the trial in 4 out of 6 experiments, and this cancer responded favorably to multi-drug therapy. CO5-1 was removed from the colon of the patient, but the location of the tumor seems to have no relevance to sensitivity in this study. Because CO5-1 was removed from the distal colon, it seems counter intuitive that the cancer responded so favorably to chemotherapy agents. In contrast, CO9-1, was one of the most insensitive cancers in our study. The tumor was removed from the proximal colon of the patient. Proximal colon mucinous adenocarcinomas typically have higher survival rates than distal mucinous adenocarcinomas³⁴. ABX 023-1 was the second most sensitive cancer, with the lowest calculated LD50 for both Oxp and Irinotecan therapy. In addition, ABX 023-1 was recorded to have the second lowest calculated LD50 for both the

Irinotecan therapy and the 40,000 MMC therapy. ABX 023-1 was classified as a PMCA with signet ring cells. These two cancers are unique within this study. CO5-1 was successfully transferred from human biopsies into immuno-deficient laboratory mice, and ABX 023-1 was a PMCA cancer biopsy taken from a patient undergoing systemic antibiotic therapy. Antibiotics are shown to minimize the aggressive nature of PMCA class PMP cases⁵¹. This could be evidence to explain why ABX 023-1 responded as well as it did to chemotherapy. However, we could not draw any distinction between PMCA and DPAM drug sensitivities. In addition, our results suggest that there are no clear differences between the PMP cancers or the mucinous colorectal adenocarcinomas with respect to growth or drug sensitivity. It is unclear whether or not the mouse host for CO5-1 affected any pathological sensitivity to these chemotherapies, but the results do imply that this particular strain responds well to all chemotherapies tested. Whether or not this is the result of the mouse host is unclear.

PMP is a devastating disease. Chemotherapy agents prove to be an effective treatment strategy; however, this therapy is predicated on the stage of cancer development. Early detection of PMP is difficult, but it is no less important than other malignancies. CRS and HIPEC is shown to be an effective intervention for late stage PMP. However, due to the advanced stage of this disease invasion into surrounding tissue can occur. HIPEC is limited by the effective depth of perfusion into surrounding tissue. This is an advantage compared to systemic chemotherapy, because the concentration of agent can be safely increased in the operative theatre. This is also a disadvantage, because based on the stage of development tissue invasion by malignant cells could outpace the depth of drug perfusion or the sheer scope of cancer colonization might overwhelm the

application. If the combination of CRS and HIPEC prove unsuccessful, traditional systemic chemotherapy is also employed. Systemic chemotherapy does not allow the physician to aggressively treat the cancer in the same parameters as HIPEC. In addition, our results reinforce the unpredictable nature of agent interactions with cancer. Of the 4 unique chemotherapies in this study, only MMC and 5-FU resulted in a calculated LD50 within an acceptable clinical plasma concentration. Each of the tested agents are currently used today as part of solitary or multidrug therapies with varying levels of success. It is in bad faith to assume a predictable outcome of chemotherapeutic intervention based on historical literature, and, in reality, a more personalized approach is necessary to determine optimal treatment. The ability to detect and successfully treat PMP prior to significant tissue invasion is paramount to patient health, however effective treatment relies on exhaustive studies like ours. Our study is not intended as the final page for PMP chemotherapy interactions, but rather another chapter to be utilized in the fight.

WORKS CITED

1. Bagheri M, Tabatabae Far MA, Mirzaei H, Ghasemi F. Evaluation of antitumor effects of aspirin and LGK974 drugs on cellular signaling pathways, cell cycle and apoptosis in colorectal cancer cell lines compared to oxaliplatin drug. *Fundam Clin Pharmacol.* 2020;34(1):51-64. Epub 2019/07/16. doi: 10.1111/fcp.12492. PubMed PMID: 31233627.
2. Bano N, Najam R, Qazi F, Mateen A. Clinical Features of Oxaliplatin Induced Hypersensitivity Reactions and Therapeutic Approaches. *Asian Pac J Cancer Prev.* 2016;17(4):1637-41. doi: 10.7314/apjcp.2016.17.4.1637. PubMed PMID: 27221832.
3. Bevan KE, Mohamed F, Moran BJ. Pseudomyxoma peritonei. *World J Gastrointest Oncol.* 2010;2(1):44-50. doi: 10.4251/wjgo.v2.i1.44. PubMed PMID: 21160816; PubMed Central PMCID: PMC2999154.
4. Bos JL. ras oncogenes in human cancer: a review. *Cancer Res.* 1989;49(17):4682-9. PubMed PMID: 2547513.
5. Casale F, Canaparo R, Serpe L, Muntoni E, Pepa CD, Costa M, et al. Plasma concentrations of 5-fluorouracil and its metabolites in colon cancer patients. *Pharmacol Res.* 2004;50(2):173-9. doi: 10.1016/j.phrs.2004.01.006. PubMed PMID: 15177306.
6. Catimel G, Chabot GG, Guastalla JP, Dumortier A, Cote C, Engel C, et al. Phase I and pharmacokinetic study of irinotecan (CPT-11) administered daily for three consecutive days every three weeks in patients with advanced solid tumors. *Ann Oncol.* 1995;6(2):133-40. doi: 10.1093/oxfordjournals.annonc.a059108. PubMed PMID: 7786821.
7. Chabot GG. Clinical pharmacokinetics of irinotecan. *Clin Pharmacokinet.* 1997;33(4):245-59. doi: 10.2165/00003088-199733040-00001. PubMed PMID: 9342501.
8. Cotte E, Passot G, Tod M, Bakrin N, Gilly FN, Steghens A, et al. Closed abdomen hyperthermic intraperitoneal chemotherapy with irinotecan and mitomycin C: a phase I study. *Ann Surg Oncol.* 2011;18(9):2599-603. Epub 2011/03/19. doi: 10.1245/s10434-011-1651-1. PubMed PMID: 21424369.
9. Darnis E, Ronceray J, Grosieux P, Soutoul JH. [Pseudomyxoma peritonei in females. 13 personal cases. Practical deductions from a review of 420 cases in the literature]. *J Gynecol Obstet Biol Reprod (Paris).* 1987;16(3):343-53. PubMed PMID: 3598100.

10. de Man FM, Goey AKL, van Schaik RHN, Mathijssen RHJ, Bins S. Individualization of Irinotecan Treatment: A Review of Pharmacokinetics, Pharmacodynamics, and Pharmacogenetics. *Clin Pharmacokinet*. 2018;57(10):1229-54. doi: 10.1007/s40262-018-0644-7. PubMed PMID: 29520731; PubMed Central PMCID: PMC6132501.
11. den Hartigh J, McVie JG, van Oort WJ, Pinedo HM. Pharmacokinetics of mitomycin C in humans. *Cancer Res*. 1983;43(10):5017-21. PubMed PMID: 6411336.
12. Dilruba S, Kalayda GV. Platinum-based drugs: past, present and future. *Cancer Chemother Pharmacol*. 2016;77(6):1103-24. Epub 2016/02/17. doi: 10.1007/s00280-016-2976-z. PubMed PMID: 26886018.
13. Drewinko B, Freireich EJ, Gottlieb JA. Lethal activity of camptothecin sodium on human lymphoma cells. *Cancer Res*. 1974;34(4):747-50. PubMed PMID: 4814992.
14. el-Deiry WS, Tokino T, Velculescu VE, Levy DB, Parsons R, Trent JM, et al. WAF1, a potential mediator of p53 tumor suppression. *Cell*. 1993;75(4):817-25. doi: 10.1016/0092-8674(93)90500-p. PubMed PMID: 8242752.
15. Forcello NP, Khubchandani S, Patel SJ, Brahaj D. Oxaliplatin-induced immune-mediated cytopenias: a case report and literature review. *J Oncol Pharm Pract*. 2015;21(2):148-56. Epub 2014/02/05. doi: 10.1177/1078155213520262. PubMed PMID: 24500808.
16. Fujimoto S, Takahashi M, Kobayashi K, Kure M, Masaoka H, Ohkubo H, et al. Combined treatment of pelvic exenterative surgery and intra-operative pelvic hyperthermochemotherapy for locally advanced rectosigmoid cancer: report of a case. *Surg Today*. 1993;23(12):1094-8. doi: 10.1007/BF00309101. PubMed PMID: 8118126.
17. Furukawa T, Kuboki Y, Tanji E, Yoshida S, Hatori T, Yamamoto M, et al. Whole-exome sequencing uncovers frequent GNAS mutations in intraductal papillary mucinous neoplasms of the pancreas. *Sci Rep*. 2011;1:161. Epub 2011/11/18. doi: 10.1038/srep00161. PubMed PMID: 22355676; PubMed Central PMCID: PMC3240977.
18. Giacchetti S, Perpoint B, Zidani R, Le Bail N, Faggiuolo R, Focan C, et al. Phase III multicenter randomized trial of oxaliplatin added to chronomodulated fluorouracil-leucovorin as first-line treatment of metastatic colorectal cancer. *J Clin Oncol*. 2000;18(1):136-47. doi: 10.1200/JCO.2000.18.1.136. PubMed PMID: 10623704.
19. Goldberg RM, Erlichman C. Irinotecan plus 5-FU and leucovorin in advanced colorectal cancer: North American trials. *Oncology (Williston Park)*. 1998;12(8 Suppl 6):59-63. PubMed PMID: 9726093.

20. Graham MA, Lockwood GF, Greenslade D, Brienza S, Bayssas M, Gamelin E. Clinical pharmacokinetics of oxaliplatin: a critical review. *Clin Cancer Res*. 2000;6(4):1205-18. PubMed PMID: 10778943.
21. Guidos CJ, Williams CJ, Grandal I, Knowles G, Huang MT, Danska JS. V(D)J recombination activates a p53-dependent DNA damage checkpoint in scid lymphocyte precursors. *Genes Dev*. 1996;10(16):2038-54. doi: 10.1101/gad.10.16.2038. PubMed PMID: 8769647.
22. Gustavsson B, Carlsson G, Machover D, Petrelli N, Roth A, Schmoll HJ, et al. A review of the evolution of systemic chemotherapy in the management of colorectal cancer. *Clin Colorectal Cancer*. 2015;14(1):1-10. Epub 2014/11/15. doi: 10.1016/j.clcc.2014.11.002. PubMed PMID: 25579803.
23. Hanski C. Is mucinous carcinoma of the colorectum a distinct genetic entity? *Br J Cancer*. 1995;72(6):1350-6. doi: 10.1038/bjc.1995.514. PubMed PMID: 8519644; PubMed Central PMCID: PMC2034069.
24. Helderma R, Löke DR, Verhoeff J, Rodermond HM, van Bochove GGW, Boon M, et al. The Temperature-Dependent Effectiveness of Platinum-Based Drugs Mitomycin-C and 5-FU during Hyperthermic Intraperitoneal Chemotherapy (HIPEC) in Colorectal Cancer Cell Lines. *Cells*. 2020;9(8). Epub 2020/07/25. doi: 10.3390/cells9081775. PubMed PMID: 32722384; PubMed Central PMCID: PMC7464333.
25. Hildebrandt B, Wust P, Ahlers O, Dieing A, Sreenivasa G, Kerner T, et al. The cellular and molecular basis of hyperthermia. *Crit Rev Oncol Hematol*. 2002;43(1):33-56. doi: 10.1016/s1040-8428(01)00179-2. PubMed PMID: 12098606.
26. Hinson FL, Ambrose NS. Pseudomyxoma peritonei. *Br J Surg*. 1998;85(10):1332-9. doi: 10.1046/j.1365-2168.1998.00882.x. PubMed PMID: 9782010.
27. Honjo K, Hiraki T, Higashi M, Noguchi H, Nomoto M, Yoshimura T, et al. Immunohistochemical expression profiles of mucin antigens in salivary gland mucoepidermoid carcinoma: MUC4- and MUC6-negative expression predicts a shortened survival in the early postoperative phase. *Histol Histopathol*. 2018;33(2):201-13. Epub 2017/06/26. doi: 10.14670/HH-11-913. PubMed PMID: 28649694.
28. Hsiang YH, Liu LF. Identification of mammalian DNA topoisomerase I as an intracellular target of the anticancer drug camptothecin. *Cancer Res*. 1988;48(7):1722-6. PubMed PMID: 2832051.
29. Huang R, Shi XL, Wang YF, Yang F, Wang TT, Peng CX. Apatinib for treatment of a pseudomyxoma peritonei patient after surgical treatment and hyperthermic

intraperitoneal chemotherapy: A case report. *World J Clin Cases*. 2019;7(22):3881-6. doi: 10.12998/wjcc.v7.i22.3881. PubMed PMID: 31799318; PubMed Central PMCID: PMC6887607.

30. Jacquet P, Jelinek JS, Chang D, Koslowe P, Sugarbaker PH. Abdominal computed tomographic scan in the selection of patients with mucinous peritoneal carcinomatosis for cytoreductive surgery. *J Am Coll Surg*. 1995;181(6):530-8. PubMed PMID: 7582228.

31. Kaneda N, Nagata H, Furuta T, Yokokura T. Metabolism and pharmacokinetics of the camptothecin analogue CPT-11 in the mouse. *Cancer Res*. 1990;50(6):1715-20. PubMed PMID: 2306725.

32. Karapetis CS, Khambata-Ford S, Jonker DJ, O'Callaghan CJ, Tu D, Tebbutt NC, et al. K-ras mutations and benefit from cetuximab in advanced colorectal cancer. *N Engl J Med*. 2008;359(17):1757-65. doi: 10.1056/NEJMoa0804385. PubMed PMID: 18946061.

33. Kennedy KA, Rockwell S, Sartorelli AC. Preferential activation of mitomycin C to cytotoxic metabolites by hypoxic tumor cells. *Cancer Res*. 1980;40(7):2356-60. PubMed PMID: 7388797.

34. Leopoldo S, Lorena B, Cinzia A, Gabriella DC, Angela Luciana B, Renato C, et al. Two subtypes of mucinous adenocarcinoma of the colorectum: clinicopathological and genetic features. *Ann Surg Oncol*. 2008;15(5):1429-39. Epub 2008/02/27. doi: 10.1245/s10434-007-9757-1. PubMed PMID: 18301950.

35. Levine AJ. p53, the cellular gatekeeper for growth and division. *Cell*. 1997;88(3):323-31. doi: 10.1016/s0092-8674(00)81871-1. PubMed PMID: 9039259.

36. Lin YL, Ma R, Li Y. The biological basis and function of GNAS mutation in pseudomyxoma peritonei: a review. *J Cancer Res Clin Oncol*. 2020;146(9):2179-88. Epub 2020/07/22. doi: 10.1007/s00432-020-03321-8. PubMed PMID: 32700107; PubMed Central PMCID: PMC7382651.

37. Longley DB, Harkin DP, Johnston PG. 5-fluorouracil: mechanisms of action and clinical strategies. *Nat Rev Cancer*. 2003;3(5):330-8. doi: 10.1038/nrc1074. PubMed PMID: 12724731.

38. Los G, Mutsaers PH, Lenglet WJ, Baldew GS, McVie JG. Platinum distribution in intraperitoneal tumors after intraperitoneal cisplatin treatment. *Cancer Chemother Pharmacol*. 1990;25(6):389-94. doi: 10.1007/BF00686048. PubMed PMID: 2311166.

39. Luo C, Cen S, Ding G, Wu W. Mucinous colorectal adenocarcinoma: clinical pathology and treatment options. *Cancer Commun (Lond)*. 2019;39(1):13. Epub

2019/03/29. doi: 10.1186/s40880-019-0361-0. PubMed PMID: 30922401; PubMed Central PMCID: PMC6440160.

40. Mann WJ, Wagner J, Chumas J, Chalas E. The management of pseudomyxoma peritonei. *Cancer*. 1990;66(7):1636-40. doi: 10.1002/1097-0142(19901001)66:7<1636::aid-cnrcr2820660731>3.0.co;2-n. PubMed PMID: 2208015.

41. McClatchey AI, Yap AS. Contact inhibition (of proliferation) redux. *Curr Opin Cell Biol*. 2012;24(5):685-94. Epub 2012/07/24. doi: 10.1016/j.ceb.2012.06.009. PubMed PMID: 22835462.

42. Mendonsa AM, Na TY, Gumbiner BM. E-cadherin in contact inhibition and cancer. *Oncogene*. 2018;37(35):4769-80. Epub 2018/05/21. doi: 10.1038/s41388-018-0304-2. PubMed PMID: 29780167; PubMed Central PMCID: PMC6119098.

43. Misdraji J, Yantiss RK, Graeme-Cook FM, Balis UJ, Young RH. Appendiceal mucinous neoplasms: a clinicopathologic analysis of 107 cases. *Am J Surg Pathol*. 2003;27(8):1089-103. doi: 10.1097/00000478-200308000-00006. PubMed PMID: 12883241.

44. Moran BJ, Cecil TD. The etiology, clinical presentation, and management of pseudomyxoma peritonei. *Surg Oncol Clin N Am*. 2003;12(3):585-603. doi: 10.1016/s1055-3207(03)00026-7. PubMed PMID: 14567019.

45. Morera-Ocon FJ, Navarro-Campoy C. History of pseudomyxoma peritonei from its origin to the first decades of the twenty-first century. *World J Gastrointest Surg*. 2019;11(9):358-64. doi: 10.4240/wjgs.v11.i9.358. PubMed PMID: 31572561; PubMed Central PMCID: PMC6766476.

46. Nishikawa G, Sekine S, Ogawa R, Matsubara A, Mori T, Taniguchi H, et al. Frequent GNAS mutations in low-grade appendiceal mucinous neoplasms. *Br J Cancer*. 2013;108(4):951-8. Epub 2013/02/12. doi: 10.1038/bjc.2013.47. PubMed PMID: 23403822; PubMed Central PMCID: PMC3590682.

47. Noguchi R, Yano H, Gohda Y, Suda R, Igari T, Ohta Y, et al. Molecular profiles of high-grade and low-grade pseudomyxoma peritonei. *Cancer Med*. 2015;4(12):1809-16. Epub 2015/10/16. doi: 10.1002/cam4.542. PubMed PMID: 26475379; PubMed Central PMCID: PMC5123786.

48. Pavel M, Renna M, Park SJ, Menzies FM, Ricketts T, Füllgrabe J, et al. Contact inhibition controls cell survival and proliferation via YAP/TAZ-autophagy axis. *Nat Commun*. 2018;9(1):2961. Epub 2018/07/27. doi: 10.1038/s41467-018-05388-x. PubMed PMID: 30054475; PubMed Central PMCID: PMC6063886.

49. Saarinen L, Nummela P, Leinonen H, Heiskanen A, Thiel A, Haglund C, et al. Glycomic Profiling Highlights Increased Fucosylation in Pseudomyxoma Peritonei. *Mol Cell Proteomics*. 2018;17(11):2107-18. Epub 2018/08/02. doi: 10.1074/mcp.RA118.000615. PubMed PMID: 30072579; PubMed Central PMCID: PMC6210226.
50. Schubbert S, Shannon K, Bollag G. Hyperactive Ras in developmental disorders and cancer. *Nat Rev Cancer*. 2007;7(4):295-308. doi: 10.1038/nrc2109. PubMed PMID: 17384584.
51. Semino-Mora C, Testerman TL, Liu H, Whitmire JM, Studeman K, Jia Y, et al. Antibiotic treatment decreases microbial burden associated with pseudomyxoma peritonei and affects β -catenin distribution. *Clin Cancer Res*. 2013;19(14):3966-76. Epub 2013/06/06. doi: 10.1158/1078-0432.CCR-13-0616. PubMed PMID: 23743566.
52. Souglakos J, Androulakis N, Syrigos K, Polyzos A, Ziras N, Athanasiadis A, et al. FOLFOXIRI (folinic acid, 5-fluorouracil, oxaliplatin and irinotecan) vs FOLFIRI (folinic acid, 5-fluorouracil and irinotecan) as first-line treatment in metastatic colorectal cancer (MCC): a multicentre randomised phase III trial from the Hellenic Oncology Research Group (HORG). *Br J Cancer*. 2006;94(6):798-805. doi: 10.1038/sj.bjc.6603011. PubMed PMID: 16508637; PubMed Central PMCID: PMC2361370.
53. St Croix B, Sheehan C, Rak JW, Flørenes VA, Slingerland JM, Kerbel RS. E-Cadherin-dependent growth suppression is mediated by the cyclin-dependent kinase inhibitor p27(KIP1). *J Cell Biol*. 1998;142(2):557-71. doi: 10.1083/jcb.142.2.557. PubMed PMID: 9679152; PubMed Central PMCID: PMC2133056.
54. Stewart JH, Shen P, Levine EA. Intraperitoneal hyperthermic chemotherapy for peritoneal surface malignancy: current status and future directions. *Ann Surg Oncol*. 2005;12(10):765-77. Epub 2005/08/18. doi: 10.1245/ASO.2005.12.001. PubMed PMID: 16132375.
55. Sugarbaker PH. Pseudomyxoma peritonei. A cancer whose biology is characterized by a redistribution phenomenon. *Ann Surg*. 1994;219(2):109-11. doi: 10.1097/00000658-199402000-00001. PubMed PMID: 8129480; PubMed Central PMCID: PMC1243111.
56. Sugarbaker PH. Peritonectomy procedures. *Surg Oncol Clin N Am*. 2003;12(3):703-27, xiii. doi: 10.1016/s1055-3207(03)00048-6. PubMed PMID: 14567026.
57. Sugarbaker PH. New standard of care for appendiceal epithelial neoplasms and pseudomyxoma peritonei syndrome? *Lancet Oncol*. 2006;7(1):69-76. doi: 10.1016/S1470-2045(05)70539-8. PubMed PMID: 16389186.

58. Sulkin TV, O'Neill H, Amin AI, Moran B. CT in pseudomyxoma peritonei: a review of 17 cases. *Clin Radiol*. 2002;57(7):608-13. doi: 10.1053/crad.2002.0942. PubMed PMID: 12096860.
59. Symonds DA, Vickery AL. Mucinous carcinoma of the colon and rectum. *Cancer*. 1976;37(4):1891-900. doi: 10.1002/1097-0142(197604)37:4<1891::aid-cnrcr2820370439>3.0.co;2-z. PubMed PMID: 177180.
60. Taguchi T, Tsukagoshi S, Furue H, Niitani H, Noda K. [Phase I clinical study of oxaliplatin]. *Gan To Kagaku Ryoho*. 1998;25(12):1899-907. PubMed PMID: 9797812.
61. Tan C, Du X. KRAS mutation testing in metastatic colorectal cancer. *World J Gastroenterol*. 2012;18(37):5171-80. doi: 10.3748/wjg.v18.i37.5171. PubMed PMID: 23066310; PubMed Central PMCID: PMC3468848.
62. Velcich A, Augenlicht LH. Regulated expression of an intestinal mucin gene in HT29 colonic carcinoma cells. *J Biol Chem*. 1993;268(19):13956-61. PubMed PMID: 7686147.
63. Wishart DS, Feunang YD, Guo AC, Lo EJ, Marcu A, Grant JR, et al. DrugBank 5.0: a major update to the DrugBank database for 2018. *Nucleic Acids Res*. 2018;46(D1):D1074-D82. doi: 10.1093/nar/gkx1037. PubMed PMID: 29126136; PubMed Central PMCID: PMC5753335.
64. Yan TD, Cao CQ, Munkholm-Larsen S. A pharmacological review on intraperitoneal chemotherapy for peritoneal malignancy. *World J Gastrointest Oncol*. 2010;2(2):109-16. doi: 10.4251/wjgo.v2.i2.109. PubMed PMID: 21160929; PubMed Central PMCID: PMC2999163.
65. Zoetemelk M, Ramzy GM, Rausch M, Nowak-Sliwinska P. Drug-Drug Interactions of Irinotecan, 5-Fluorouracil, Folinic Acid and Oxaliplatin and Its Activity in Colorectal Carcinoma Treatment. *Molecules*. 2020;25(11). Epub 2020/06/04. doi: 10.3390/molecules25112614. PubMed PMID: 32512790; PubMed Central PMCID: PMC7321123.